NASA TECHNICAL NOTE

NASA TN D-7270

NASA TN D-7270

A TECHNIQUE FOR MEASURING HYPERSONIC FLOW VELOCITY PROFILES

by Luther R. Gartrell

Langley Research Center
Hampton, Va. 23665

NATIONAL AERONAUTICS AND SPACE ADMINISTRATION • WASHINGTON, D. C. • JULY 1973

1. Report No.	2. Government Accession No.	3. Recipient's Catalog No.
NASA TN D-7270		

4. Title and Subtitle	5. Report Date
A TECHNIQUE FOR MEASURING HYPERSONIC FLOW VELOCITY PROFILES	July 1973
	6. Performing Organization Code
7. Author(s)	8. Performing Organization Report No.
Luther R. Gartrell	L-8815
	10. Work Unit No.
9. Performing Organization Name and Address	502-07-01-07
NASA Langley Research Center Hampton, Va. 23665	11. Contract or Grant No.
	13. Type of Report and Period Covered
12. Sponsoring Agency Name and Address	Technical Note
National Aeronautics and Space Administration Washington, D.C. 20546	14. Sponsoring Agency Code

15. Supplementary Notes

16. Abstract

A technique for measuring hypersonic flow velocity profiles is described. This technique utilizes an arc-discharge—electron-beam system to produce a luminous disturbance in the flow. The time of flight of this disturbance was measured. Experimental tests were conducted in the Langley pilot model expansion tube. The measured velocities were of the order of 6000 m/sec over a free-stream density range from 1.96×10^{-4} to 1.86×10^{-3} kg/m^3. The fractional error in the velocity measurements was less than 5 percent. Long arc-discharge columns (0.356 m) were generated under hypersonic flow conditions in the expansion tube modified to operate as an expansion tunnel.

17. Key Words (Suggested by Author(s))	18. Distribution Statement
Arc discharge Flow velocity measurements	Unclassified – Unlimited

19. Security Classif. (of this report)	20. Security Classif. (of this page)	21. No. of Pages	22. Price*
Unclassified	Unclassified	38	$3.00

*For sale by the National Technical Information Service, Springfield, Virginia 22151

A TECHNIQUE FOR MEASURING HYPERSONIC FLOW VELOCITY PROFILES

By Luther R. Gartrell
Langley Research Center

SUMMARY

A technique for measuring hypersonic flow velocity profiles is described. This technique utilizes an arc-discharge—electron-beam system to produce a luminous disturbance in the flow. The time of flight of this disturbance was measured. Experimental tests were conducted in the Langley pilot model expansion tube. The measured velocities were of the order of 6000 m/sec over a free-stream density range from 1.96×10^{-4} to 1.86×10^{-3} kg/m^3. The fractional error in the velocity measurements was less than 5 percent. Long arc-discharge columns (0.356 m) were generated under hypersonic flow conditions in the expansion tube modified to operate as an expansion tunnel.

INTRODUCTION

The work presented herein was undertaken to develop a system for measuring free-stream hypersonic flow velocity profiles in expansion tube facilities. In general, velocity measurements in conventional supersonic wind tunnels can be obtained by indirect methods using aerodynamic probes to measure parameters from which the velocity can be calculated. For example, in equilibrium flow, the velocity can be obtained by measurements of total and static pressures and total temperature or total and static pressures and mass flow rate. If the flow is not in equilibrium, an additional independent measurement, such as the local temperature, is required. However, due to the inherent properties of hypersonic flows, probe techniques tend to make velocity determinations highly uncertain. The uncertainties are brought about by one or more of the following conditions:

(1) High-enthalpy level, because of high dissociation and ionization, which limits total temperature measurements

(2) The presence of a probe in the flow which disturbs the flow to an undeterminable degree

(3) Deviation of pressures from those of the actual free-stream values, as seen by the static-pressure and total-head probes

(4) Extremely high heat-transfer rates which limit the sampling test time

Numerous methods have been used by several investigators for obtaining direct velocity measurements in hypersonic streams. Kyser (ref. 1) and Bomelburg and associates (ref. 2) used a series of sparks to traverse a gas stream at a high repetition rate. The spark produced a path of momentarily ionized gas particles in the flow. These ionized particles, displaced by the gas stream, provided a preferential path for each succeeding spark to follow. Photographs were taken of the change in position of the spark path. Friesen (ref. 3) used photons to preionize the gas in a localized column to generate a preferential path for a delayed spark. The velocity profile was determined from a photograph of the displaced spark and the delay time. Karamcheti and associates (ref. 4) used schlieren photographs to detect disturbances induced by an electric-arc discharge. Freeman and associates (ref. 5) used photomultiplier tubes to detect the inherent luminosity fluctuations in plasma jets. Beasley and associates (ref. 6) made velocity measurements by producing a luminous disturbance in the gas with an electric-arc discharge and detecting it sometime later with photomultiplier tubes.

In principle, the technique described in this paper is similar to that of reference 6 with significant differences being the use of preionization and the determination of a flow velocity profile. The use of preionization allows the technique to be applied to large and slightly ionized flows, characteristic of high-enthalpy hypersonic tunnels. In addition, the profile measurement aids in determining the effective test core size. This measurement is particularly useful in expansion tube flows where the boundary-layer thickness is likely to present a problem. The technique utilizes a short-duration arc discharge, a continuous electron beam, and an array of photomultiplier tubes with associated optics. The electron beam is used to produce a preferential path for the arc discharge to follow in the test gas. In this manner, a plasma is formed which persists for approximately 50 μsec after the electric field is removed. The plasma displacement rate is assumed to be equal to the local velocity and, thus, the velocity profile of the free stream and boundary layer is obtained. In this study several simultaneous measurements had to be made during microseconds test times, and this required high system reliability. Optical techniques were used to increase the detector system sensitivity and resolution.

In order to evaluate the capability of this technique in a hypersonic environment, a system was developed and tests were conducted in the Langley pilot model expansion tube. This report describes the results of these tests.

SYMBOLS

d	distance between electrodes
E	electric field, V/m

E_o	electric field at center of arc-discharge column, V/m
H	distance from midplane to either charge (electrode)
h	simulated altitude, km
i	current at anode
i_o	initial current at cathode
p	static pressure, N/m^2
p_1	initial gas pressure in the intermediate chamber, N/m^2
p_4	initial driver gas pressure, N/m^2
p_5	wall static pressure in test section, N/m^2
p_{10}	initial gas pressure in acceleration chamber, N/m^2
r	radial distance from center line, cm
Δs	distance between entrance slits, m
Δt	time of flight, sec
U	measured velocity, m/sec
U_i	interface velocity, m/sec
V	electrode potential, volts
V_s	minimum breakdown potential, volts
$\bar{v}$	average velocity, m/sec
α	Townsend's first ionization coefficient
γ	number of secondary electrons produced by each positive ion arriving at cathode
ρ	free-stream density, kg/m^3

VELOCITY MEASUREMENT TECHNIQUE

A brief description of the arc-discharge—electron-beam photometric technique for medium flow measurement is given without elaborating on the theory involved. A schematic diagram illustrating this technique is shown in figure 1. A continuous electron beam is used to create a preferential path for the arc column. In this manner, a self-sustained arc discharge is produced between the electrodes located at the edge of the flow boundary layer. The discharge current through the gas is given by (ref. 7)

$$i = i_0 \frac{e^{\alpha d}}{1 - \gamma\left(e^{\alpha d} - 1\right)} \tag{1}$$

with Townsend's breakdown occurring when

$$\gamma\left(e^{\alpha d} - 1\right) = 1 \tag{2}$$

and it is limited by the external supply.

In equations (1) and (2), α is Townsend's first ionization coefficient, d is the distance between electrodes, and γ is the number of secondary electrons produced by each positive ion on the way to the cathode.

As a result of the foregoing process, a luminous disturbance is created in the flow. The displacement of this disturbance is related to the velocity profile. A time-of-flight measurement is made as this disturbance moves downstream past a pair of photodetectors. The resulting output is recorded on a dual beam oscilloscope. A typical trace of the output is shown in figure 2. The waveform represents the intensity distribution of the residual luminous region as it passes the image slits. The shift in the peak position Δt corresponds to the time of flight over a distance Δs. By using this time and the precalibrated distance of separation between the image slits Δs, an average velocity can be calculated as follows:

$$\overline{v} = \frac{\Delta s}{\Delta t} \tag{3}$$

Shown in figure 3 is a simplified diagram illustrating the 7×2 matrix photodetector apparatus used to measure velocities in the adjacent regions of the medium for determining the flow velocity profile. This technique has been used in hypersonic flows with free-stream densities ranging from 1.96×10^{-4} to 1.86×10^{-3} kg/m^3.

DEVELOPMENT OF THE ARC-DISCHARGE—ELECTRON-BEAM SYSTEM

The gaseous plasma created as a result of an arc discharge is utilized as a tracer for measuring gas velocities. Three assumptions are essential to this technique. First,

the plasma propagates with stream velocity. Second, the point where the peak light intensity occurs during the decaying plasma process remains constant relative to the plasma. Third, the plasma intensity decay time is long compared with its image traversal time across either slit. Because of the second assumption and for improving the spatial resolution, it is desirable to restrict the arc discharge to the narrowest possible path width. The path shape depends on the electric-field distribution. For example, let a pair of small electrodes be approximated by a pair of opposite charges as shown in figure 4. The equation describing the electric field is given by (ref. 1)

$$\frac{E}{p} = \frac{E_0}{p}\left[\frac{1}{1 + \left(\frac{r}{H}\right)^2}\right]^{3/2}$$

where p is the static pressure, r is the radial distance from the center line, and H is the distance from the midplane to either charge. Factors influencing the electric-field distribution are (1) the arc-discharge electrode configuration and spacing, (2) the state of excitation and ionization of the propagation medium, and (3) the shape and material of the tunnel surroundings, which generally cannot be changed. Development work discussed in this section covers steps taken to deal with items (1) and (2). First is discussed the selection of an electrode configuration; this is followed by a discussion of the advantages associated with preionization techniques using an electron beam.

The initial electrode design work was carried out in the laboratory. Emphasis was placed on the cathode because it emitted the main current carriers of the arc discharge (electrons). For electrode spacing greater than 0.07 m, the shape of the anode had little effect on the field pattern in the vicinity of the cathode.

The electrostatic-field pattern was obtained by an electroconductive analog method. There are three forms of this method: namely, thin alloy plates with brass or copper electrodes, electrolytic tank, and surface-conducting sheets with painted electrodes. The third form was found to be more expedient for obtaining a cross section of the field patterns for various electrode configurations. Where three-dimensional Laplacian fields are to be determined, which normally require the use of an electrolytic tank, surface-conducting paper can be used provided the appropriate modifications are made. (See refs. 8 and 9.) Since the electric-field pattern data presented in this report were used only for approximation purposes, the two-dimensional configuration was investigated by using the surface-conducting paper method. This method required the use of carbon-filled analog mapping paper, which simulated an initial charge-free region at high vacuum conditions. Various electrode configurations were sketched on this paper by using conducting aluminum lacquer. Next, a potential difference, scaled to duplicate operating conditions, was applied to the electrodes. By use of a digital voltmeter, the equipotential lines were located. After obtaining the equipotential lines, the flux lines were approximated by drawing them normal to the equipotential lines. Shown in figures 5(a) and 5(b)

are idealized fields for the pointed electrodes and the concave cone-shaped cathode, respectively. The latter configuration was used since it produced paraxial flow of electrons and ions. The behavior of a charged particle in the presence of an electric field and gas molecules involves many complexities not evident in the simple theory. Such calculations require information about the mean cross section for collision between the charged particles in the presence of gas molecules. The mean cross section involves ionization, elastic scattering, and excitation contributions, with a strong dependence on the energy of the charged particle. In the absence of this detailed information, the distribution of the charges was determined experimentally by photographing the arc column in air.

The selection of the material for the cathode was based on its work function and availability. Regardless of the emission process active at the cathode – namely, positive ion bombardment, photoemission, thermoemission, or all occurring simultaneously – the low-work function surfaces have a higher electron emission than the high-work function surfaces. On this basis, aluminum was selected for the electrode design.

The cathode shape was annular so that an electron beam could be used in conjunction with the arc discharge. The electron beam helped to confine the arc column, particularly at the large electrode spacing. It increased the ionization efficiency and the space charge distribution by producing excited and ionized states along the center of the arc column. An increase in ionization efficiency is realizable because the ionization cross section for initially excited atoms may be larger than that for the atoms in the ground state. (A discussion of this process is given in ref. 7.)

Clarke and Hutton (ref. 10) conducted experiments for reducing the voltage required for breakdown across a plane gap, by passing a beam of high-energy electrons (1 MeV). As a result, a lower breakdown voltage was obtained in the presence of the electron beam. As the intensity of the beam was increased, thus increasing the initial ionization, the breakdown voltage decreased to approximately 1/5 of the value without the beam. Space charge distortion, due to the presence of the positive ions produced by the beam of electrons, is responsible for the above effect. This is because the positive ions remain longer in the gap due to their relative low mobility.

An additional discussion on the effect of space-charge distortion is given in reference 11. The author points out that for a well-defined minimum point P_0 on the gas electrical breakdown curve (Paschen's), the effect of space-charge distortion is not the same on both sides of this point. For example, the presence of positive space charge causes a decrease in the original gap length d_0 to an effective gap length d_1. With reference to sketch (a), it can be seen that to the right of the minimum point P_0 and for a given pressure p, a decrease in the effective gap length reduces the required voltage for breakdown. However, to the left of this point, the opposite effect takes place. Therefore, for large values of pd, space-charge distortion is desirable.

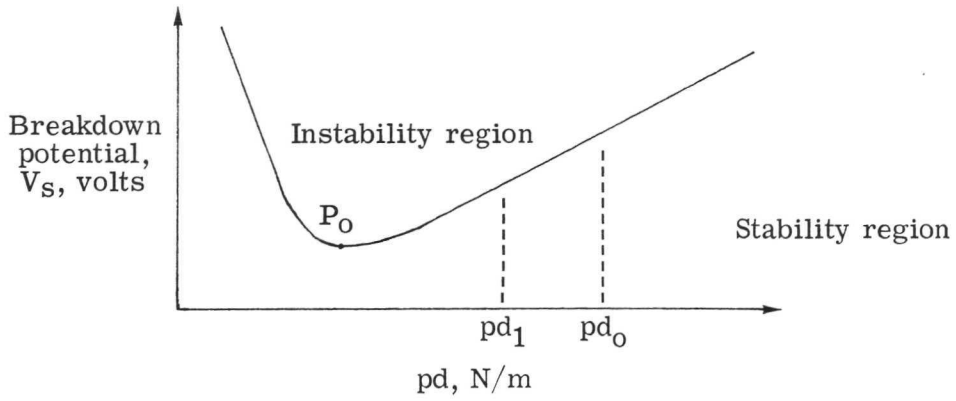

Sketch (a)

The initial tests of the arc-discharge—electron-beam system were conducted in the laboratory. These tests were made under various density conditions to cover the expected operating range in the expansion tube and expansion tunnel, a modified version of the expansion tube. The electrode spacings were adjusted accordingly. Several photographs were taken of the arc column with and without the electron beam. For each test configuration, the same exposure conditions – that is, gas density, aperture setting, and shutter speed – were maintained. In this way, an allowance could be made for the variation in the film density and processing. Densitometer traces of the film were made and the results indicated the same general trend as shown in figure 6. In each of the tests, the arc column associated with the electron beam was more confined.

EXPERIMENTAL APPARATUS

In order to evaluate the system in a hypersonic environment, tests were conducted in the Langley pilot model expansion tube. A schematic diagram of this facility is shown in figure 7(a). For a detailed description of this facility, see references 12 and 13. The expansion tube was modified to operate as an expansion tunnel by installing a nozzle in the dump tank section. (See fig. 7(b).)

The velocity measuring apparatus installed in the expansion tube is shown in figure 8. A diagram for the electron gun and the electrodes mounted in the test section of the expansion tube is shown in figure 9. A detailed discussion of the design and construction of the electrode system was given in the previous section. The electron gun, shown in figure 10, has a directly heated cathode. The electrons from the cathode are accelerated by the potential difference between the cathode and the anode chamber. Magnetic focusing and deflection coils were used to direct the electrons from the cathode through a 1.02-mm-diameter aperture. The operating conditions for the gun required the pressure in the gun chamber to be less than 1.33×10^{-2} N/m^2. Typical electron acceleration voltages were of the order of 25 kV, with electron beam currents ranging from 0.3 to 1 mA.

A circuit diagram of the pulsed energy source (arc-discharge apparatus) is shown in figure 11. This apparatus consists of a 5C22 thyratron, a 0.2-μF capacitor, a 0- to 10-kV power supply, and a trigger unit. Major components of the trigger unit are a 4C35 thyratron, a 0.1-μF capacitor, and a 20:1 pulse transformer. This unit provided ground isolation for the main discharge circuit. The output energy from the arc-discharge apparatus was variable to 10 J, with a peak current of 10^3 A. For the measurements discussed in this paper, the output energy and current were 3.6 J and 800 A (peak), respectively. The inherent system delay after the trigger signal was less than 2 μsec with a pulse duration time of the order of 1 μsec.

The detector system, shown in figures 12 and 13, was designed to observe the passing of the plasma in the flow. To assure the alinement of the system with respect to the flow, it was mounted directly to the wall of the test section. It is a 14-channel device, capable of measuring seven discrete velocities across the flow independently during a given run. The distance of separation between the slits could be varied from 1.27 cm to 3.08 cm in steps of 1.27 cm. The system housed an f/6.8 lens of 0.08189 m focal length which was used to image the induced light onto 0.154-mm-diameter entrance slits with unity magnification. Flexible light guides, 6.35 mm in diameter, were equally spaced 1.27 cm along the entrance slits. They were used to transmit the light from the entrance slits to the photocathode surfaces of the photomultiplier tubes (931-A). During the time of the arc discharge, the photodetectors were exposed to high background levels. In order to obtain the response necessary for detecting a signal at the stations located adjacent to the arc electrodes, the photomultiplier tubes were terminated by a 470-Ω load resistor (R_L); all other load resistors were 4.7 kΩ. In addition, the length of the cables was kept as short as possible. A wiring diagram for the photomultiplier base is shown in figure 14.

EXPERIMENTAL PROCEDURE

The experimental tests were conducted in two parts: (1) measurements of flow velocity profiles in the expansion tube and (2) tests in the expansion tunnel to demonstrate the system capability of operating at large electrode spacing under hypersonic flow conditions, such as are required in the Langley hot gas radiation research facility.

The following procedure was carried out for making flow-velocity-profile measurements in the expansion tube. The electron gun, operating at 25 kV, was adjusted so that a beam current of the order of 0.3 mA or better could be obtained. The 0.2-μF capacitor in the arc-discharge apparatus, initially charged to 6 kV, was discharged along a path created by the electron beam in the desired portions of the test gas through the use of appropriate time delays. Because of the short test time ($\approx$100 μsec) of the Langley pilot model expansion tube, this apparatus was electronically synchronized to the flow by using the scheme shown in figure 15. The location of the pressure sensor relative to the test

section and its output waveform are shown in figures 16(a) and 16(b), respectively. The time for the test gas to reach the test section was determined from the estimated flow velocity for a given test condition. At the helium-air interface region, there existed ionization which tended to create a preferential path from the arc discharge. This problem was eliminated by delaying the trigger to the arc-discharge apparatus long enough to allow the helium-air interface to move far enough downstream. The oscilloscope monitoring the pressure sensor output was operated in the single-sweep mode to avoid possible recycling of the arc discharge caused by noise pickup at the end of the test time. By using the 7×2 matrix detector system, seven simultaneous independent velocity measurements were made during each run.

A schematic diagram of the experimental setup in the expansion tunnel is shown in figure 17. Photographs of the apparatus and of the electrodes installed in the test section of the expansion tunnel are shown in figures 18 and 19, respectively. The electrodes were spaced approximately 0.355 m apart. For this phase of the experimental tests, only photographs were taken of the arc under flow conditions.

TEST CONDITIONS

The desired range of the test density for a given pressure p_1 in the intermediate chamber and driver gas pressure p_4 was obtained by varying the pressure in the intermediate chamber p_{10}. A detailed discussion of this process is given in references 12 and 13. The test conditions in the expansion tube for the flow-velocity-profile measurements discussed herein are given in the following table:

Test gas	p_1, N/m^2	p_{10}, N/m^2	U_i, m/s	ρ, kg/m^3	h, km
Air	2930	0.133	6052	1.96×10^{-4}	63.0
Air	2930	.665	6091	3.91×10^{-4}	58.0
Air	2930	1.33	5973	7.53×10^{-4}	52.5
Air	2930	6.65	5138	1.86×10^{-3}	45.4

The conditions for various runs could be closely duplicated. The effective test time for the tests conditions was of the order of 100 μsec.

In the expansion tunnel, tests were made with $p_{10} = 133$, 110, and 66.5 N/m^2. The test gas (air) pressure in the intermediate chamber was 2930 N/m^2.

SYSTEM ACCURACY

The accuracy of the flow velocity measurement system depends primarily on the precision with which distance between the detectors and the time of flight can be determined.

Two methods were used to determine the distance between the detectors: (1) Measurement of the physical separation of the entrance slits and (2) dynamic calibration of the entire detector system which took into account the differing photocathode sensitivity for each of the detectors. This calibration was performed by mounting a point light source, approximately 0.04 cm in diameter, on the plotting arm of an x-y recorder which had the capability to sweep in the x-direction at a constant rate. As the light source moved past the detectors, the outputs from the detectors were connected to the y-input of the x-y recorder. The recorder output was in the form of distinct peaks displaced on the X-axis. A number of measurements were taken and the results indicated that the distance of separation of the detectors could be determined within ± 0.5 percent.

Other factors that influence the time-of-flight measurement are the accuracy of the oscilloscope sweep rate and the ability to measure the time interval between the pulses from the oscilloscope records. The sweep rate accuracy, checked periodically, was found to be within ± 1 percent. The time interval measurement was dependent on the velocity. Over the range of velocities measured, the oscilloscope traces could be resolved to ± 0.2 μsec. The overall rms error was of the order of 5 percent.

RESULTS AND DISCUSSION

Flow-velocity-profile measurements were made in the Langley pilot model expansion tube with velocities of the order of 6000 m/sec and free-stream densities ranging from 1.96×10^{-4} to 1.86×10^{-3} kg/m^3. The results of these measurements are given in figure 20, which shows the velocity profile approximately 50 μsec behind the helium-air interface at various run conditions. A constant velocity, within 20 percent, over 80 percent of the diameter was indicated at the test section. The measured velocities were compared with the velocity of the helium-air interface obtained by microwave interferometer techniques. For velocities in a 30 percent region relative to the center-line value, the microwave measurements and the present data agreed within 5 percent for the entire range of experimental conditions.

From the aforementioned experimental results, an upper operating density limit of the order of 1.86×10^{-3} kg/m^3 was established. Although it was possible to generate an arc discharge at much higher densities, the measurement was limited due to the decreased persistence time in the plasma afterglow. Ideally, the solution would be to move the detector system closer upstream toward the electrodes. However, this distance was limited by the system recovery time after being exposed to high background levels generated by the initial arc discharge.

The lowest operating density for which measurements were attempted was of the order of 1.96×10^{-4} kg/m^3. This density was the lower operating limit for the test facility. However, results of laboratory experiments indicated that an arc discharge

could be generated at densities of the order of 2.54×10^{-5} kg/m^3. Earlier laboratory experimental results have indicated that the persistence time of the plasma afterglow varies inversely with density. From these results, it is suspected that flow velocity measurements could be made in this density range. The densities given in the paper are approximate values based on certain assumptions about the expanded gas, pitot-pressure measurements, and velocities in a hypersonic flow regime.

In the expansion tunnel, the arc column was photographed under flow conditions. The photograph shown as figure 21(a) was taken without the presence of the electron beam and reveals an apparent distortion in the arc column. The most likely reason for this distortion is the presence of an ionized region in the test gas, with charge densities high enough to cause a substantial redistribution of the energy in the arc column. For example, in expansion tube hypersonic flows with air as a test gas, ionized atoms are present. The ionization rates behind a high-speed shock wave are discussed in reference 14, where it is pointed out that over a shock velocity range between 4000 and 7000 m/sec, with air as a test gas, the dominant ionization mechanism is the reaction $N + O \rightarrow NO^+ + e$. For the expansion tube utilized for the tests discussed in this report, photomultiplier tubes were used to detect the radiation (light) at the helium-air interface and in the test gas (ref. 12). This verified the existence of excited and probably ionized states in the test gas.

The distortion was minimized by confining the energy in the arc column to a small cross-sectional area, that is, a reduced volume for a given arc column length. This was accomplished by the use of an electron beam. The photograph presented as figure 21(b) and taken under conditions similar to those of figure 21(a) shows the electron beam in conjunction with the arc discharge. The results clearly demonstrate the capability of the arc-discharge—electron-beam system to generate a relatively long arc-discharge column (0.36 m) in a hypersonic environment. Normalization of the intensity profile shown in figure 6 to peak values provides an improvement in spatial resolution of approximately 50 percent with preionization and the annular cathode.

CONCLUDING REMARKS

An arc-discharge—electron-beam photometric technique for measuring hypersonic flow velocity profiles has been investigated. A system has been designed, constructed, and used to measure free-stream flow velocity profiles in the Langley pilot model expansion tube. In addition, it has been demonstrated that the system could generate relatively long arc-discharge columns (0.36 m) in a hypersonic environment. On the basis of the results obtained, the following significant observations can be made:

1. Flow-velocity-profile measurements can be made in a hypersonic flow at approximately 6000 m/sec with free-stream densities ranging from 1.96×10^{-4} to 1.86×10^{-3} kg/m^3.

2. By using the electron beam as a preionization source, the measurement technique can be extended to large (0.36 m) test cores.

3. Velocity measurements can be made with an overall rms error of the order of 5 percent.

4. The lens-type detector system offers excellent resolution and sensitivity capabilities. It is particularly useful at the lower free-stream densities where low intensity measurements are experienced.

Langley Research Center,
National Aeronautics and Space Administration,
Hampton, Va., May 30, 1973.

REFERENCES

1. Kyser, James B.: Additional Study and Further Development of the Tracer-Spark Technique for Flow-Velocity Measurements – A Study of the Structure of Spark Columns for Velocity Measurement in a Hypersonic Stream. NASA CR-760, 1967.

2. Bomelburg, H. J.; Herzog, J.; and Weske, J. R.: The Electric Spark Method for Quantitative Measurements in Flowing Gases. Tech. Note BN-157 (AFOSR TN-59-273, AD 212 707), Inst. Fluid Dyn. & Appl. Math., Univ. of Maryland, Jan. 1960.

3. Friesen, Wilfred J.: Use of Photoionization in Measuring Velocity Profile of Free-Stream Flow in Langley Pilot Model Expansion Tube. NASA TN D-4936, 1968.

4. Karamcheti, Krishnamurty; Vali, Walter; Kyser, James B.; and Rasmussen, Maurice L.: Measurements of Pressure and Speed of Flow in a Spark-Heated Hypersonic Wind Tunnel. AEDC-TDR-62-218, U.S. Air Force, Nov. 1962. (Available from DDC as AD 288 668.)

5. Freeman, Mark P.; Li, Sik U.; and Von Jaskowsky, W.: Velocity of Propagation and Nature of Luminosity Fluctuations in a Plasma Jet. J. Appl. Phys., vol. 33, no. 9, Sept. 1962, pp. 2845-2848.

6. Beasley, W. D.; Brooks, J. D.; and Barger, R. L.: Direct Velocity Measurements in Low-Density Plasma Flows. NASA TN D-1783, 1963.

7. Von Engel, A.: Ionized Gases. Second ed., Clarendon Press (Oxford), 1965.

8. Sherry, N. P. R.; and Curtis, A. R.: An Analogue Transformation Method of Obtaining Stream-Lines in Problems Having Axial Symmetry. Brit. J. Appl. Phys., vol. 14, no. 5, May 1963, pp. 310-311.

9. Vitkovitch, D., ed.: Field Analysis. D. Van Nostrand Co., Ltd., c.1966.

10. Clarke, J. D.; and Hutton, P. J.: Triggering of Undervolted Spark Gaps by a Microsecond Pulse of Fast Electrons. Comptes Rendus de la VI^{e} Conférence Internationale sur les Phénomènes d'Ionisation dans les Gaz (Paris), Vol. II, P. Hubert and E. Crémieu-Alcan, eds., 1963, pp. 347-351.

11. Cobine, James Dillon: Gaseous Conductors. McGraw-Hill Book Co., Inc., 1941.

12. Jones, Jim J.; and Moore, John A.: Exploratory Study of Performance of the Langley Pilot Model Expansion Tube With a Hydrogen Driver. NASA TN D-3421, 1966.

13. Trimpi, Robert L.: A Preliminary Theoretical Study of the Expansion Tube, a New Device for Producing High-Enthalpy Short-Duration Hypersonic Gas Flows. NASA TR R-133, 1962.

14. Wilson, J.: Ionization Rate of Air Behind High-Speed Shock Waves. Phys. Fluids, vol. 9, no. 10, Oct. 1966, pp. 1913-1921.

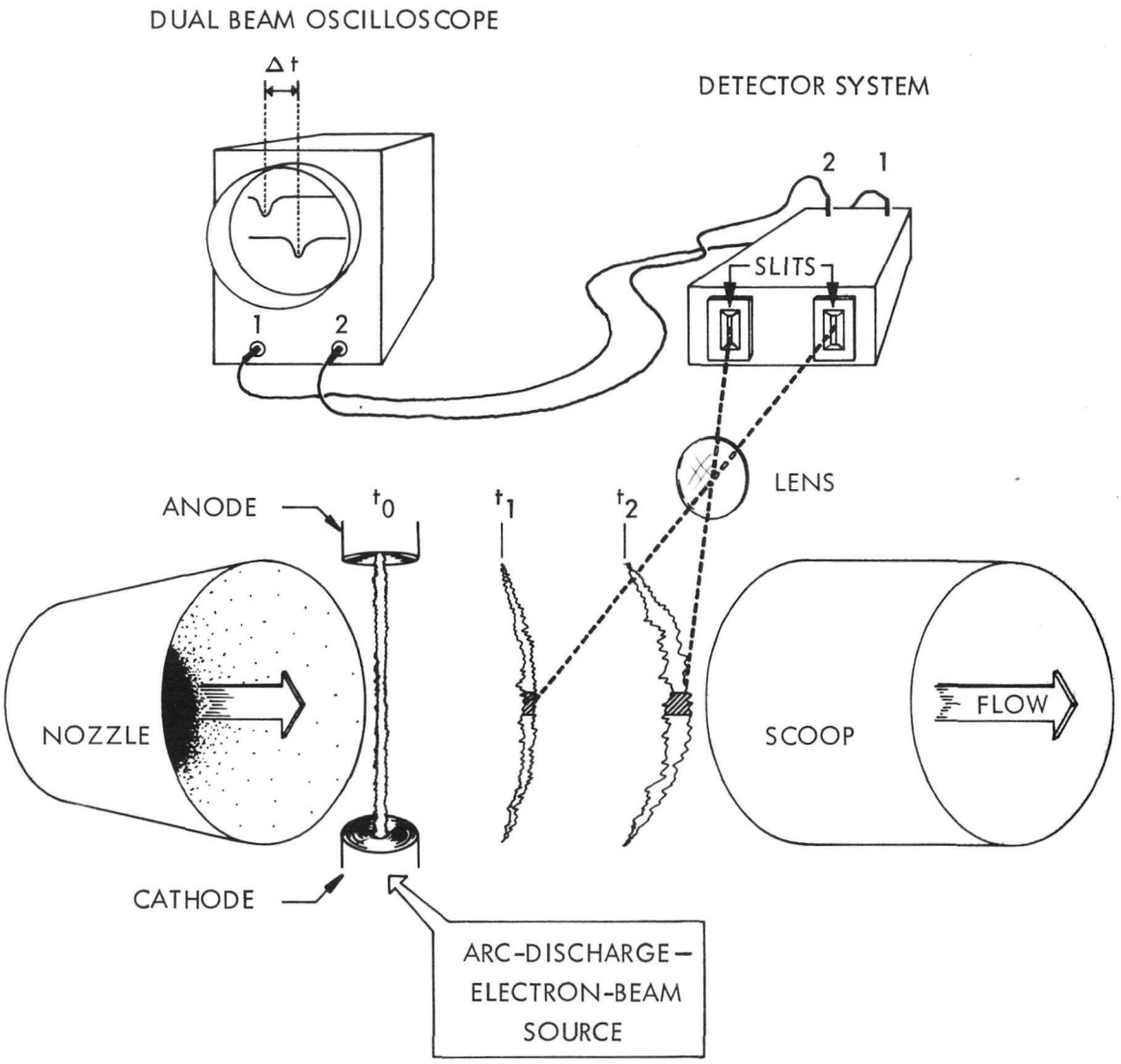

Figure 1.- Simplified diagram of the arc-discharge—electron-beam photometric technique.

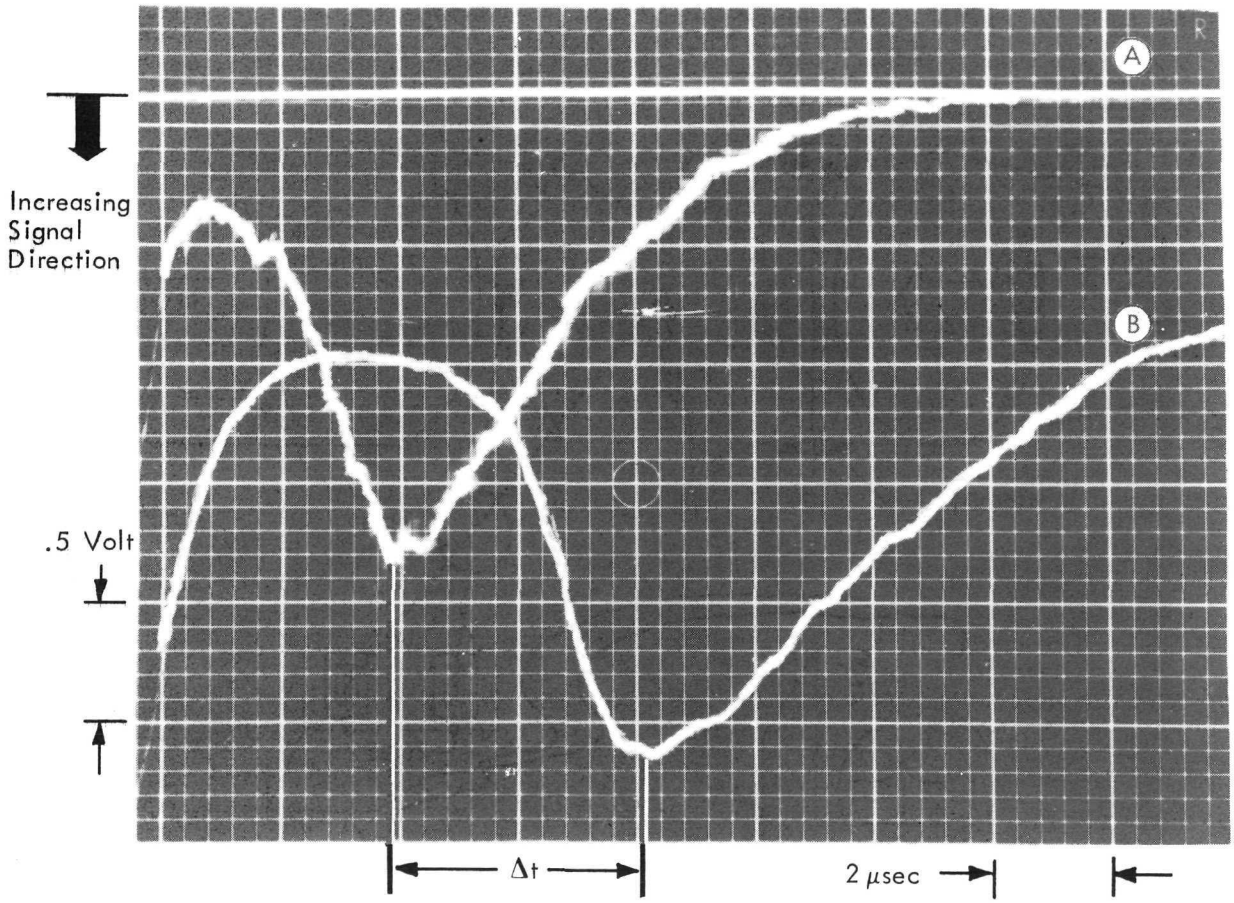

L-73-3082

Figure 2.- Typical oscilloscope record for two of the channels of the detector system.

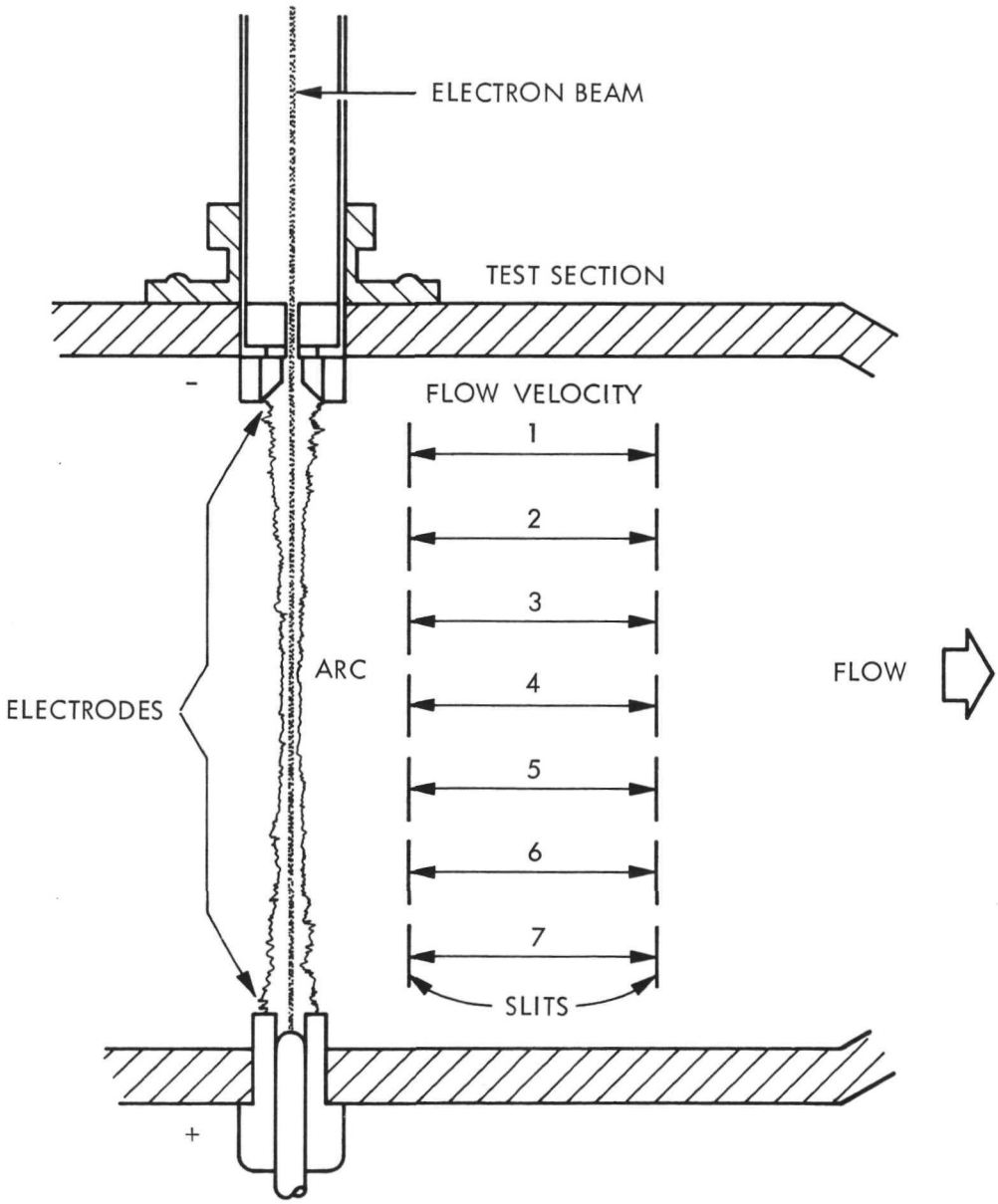

Figure 3.- Illustration of the detector matrix for measuring flow velocity profiles.

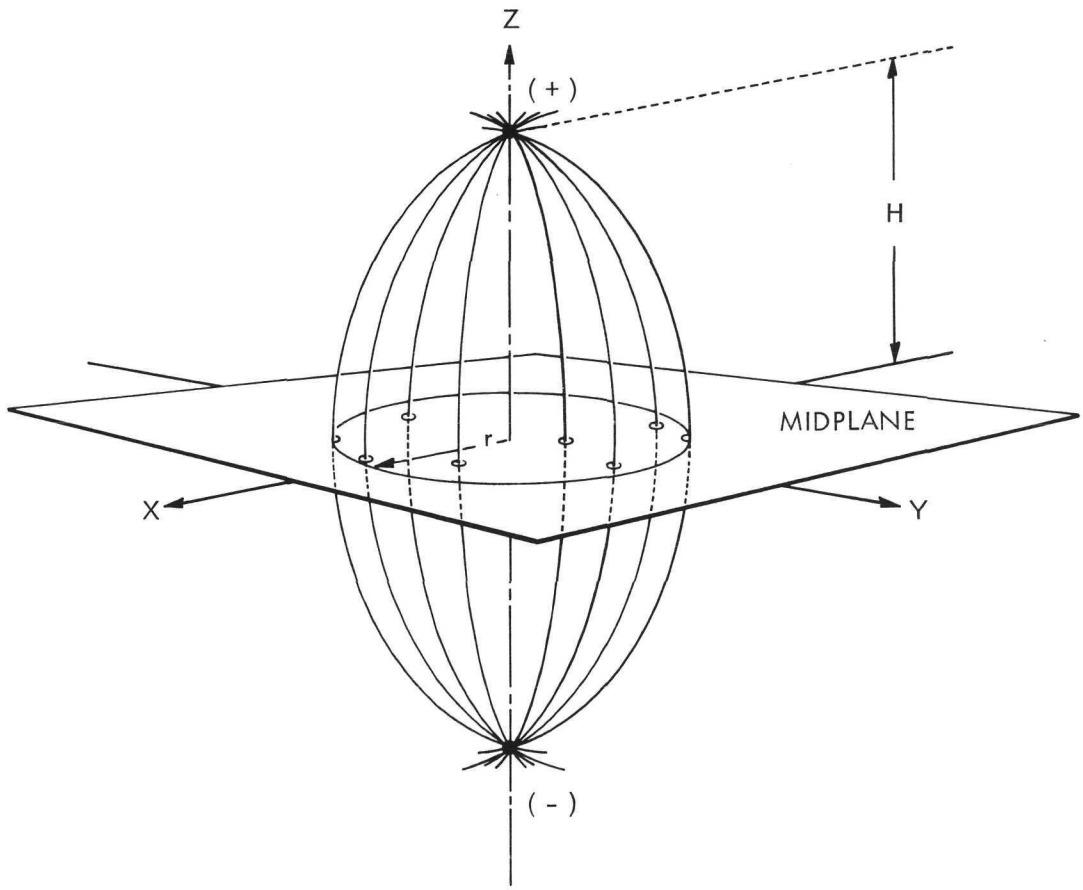

Figure 4.- Electric field between point charges of opposite polarity.

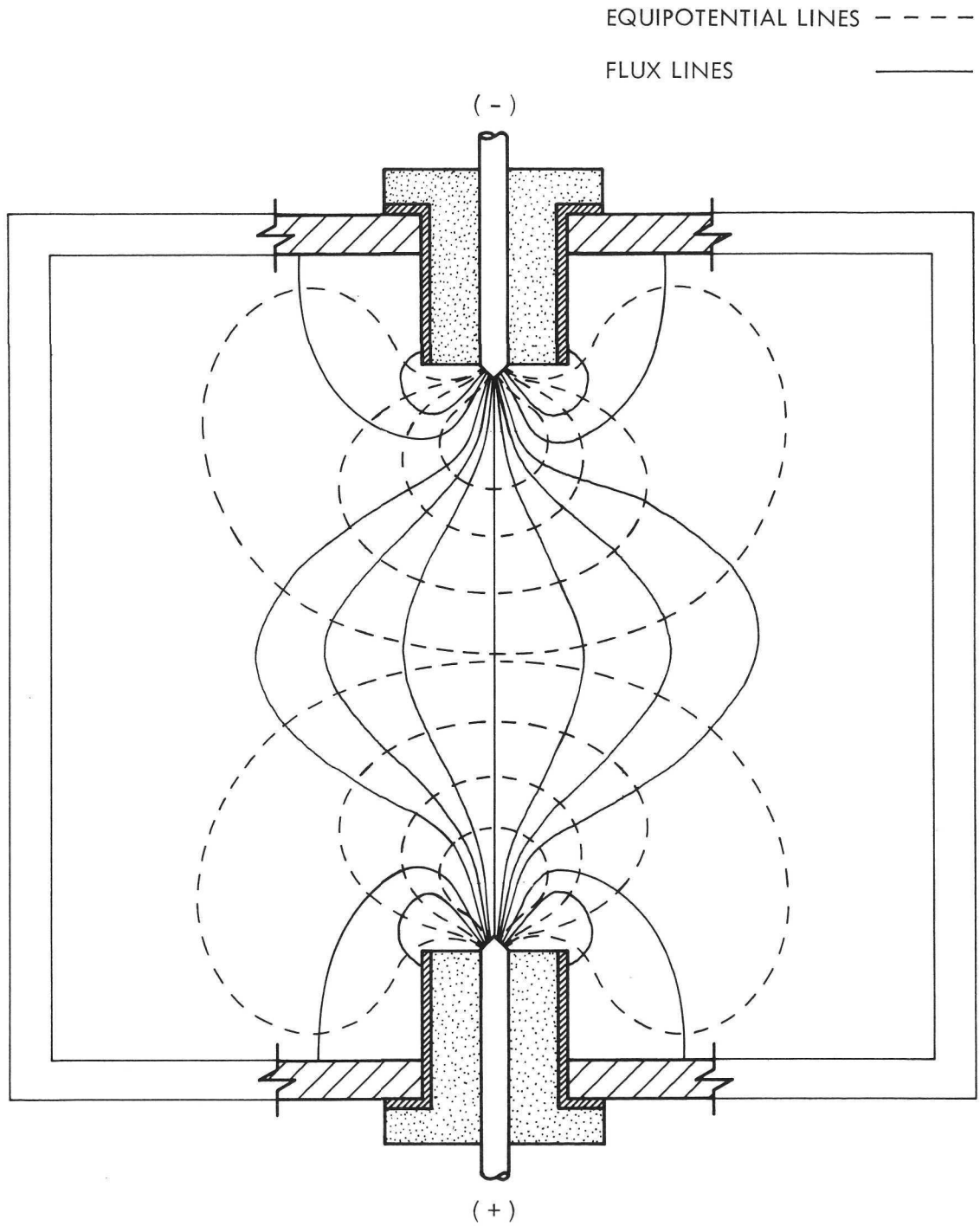

(a) Field of pointed electrodes.

Figure 5.- Electric fields for various electrode configurations.

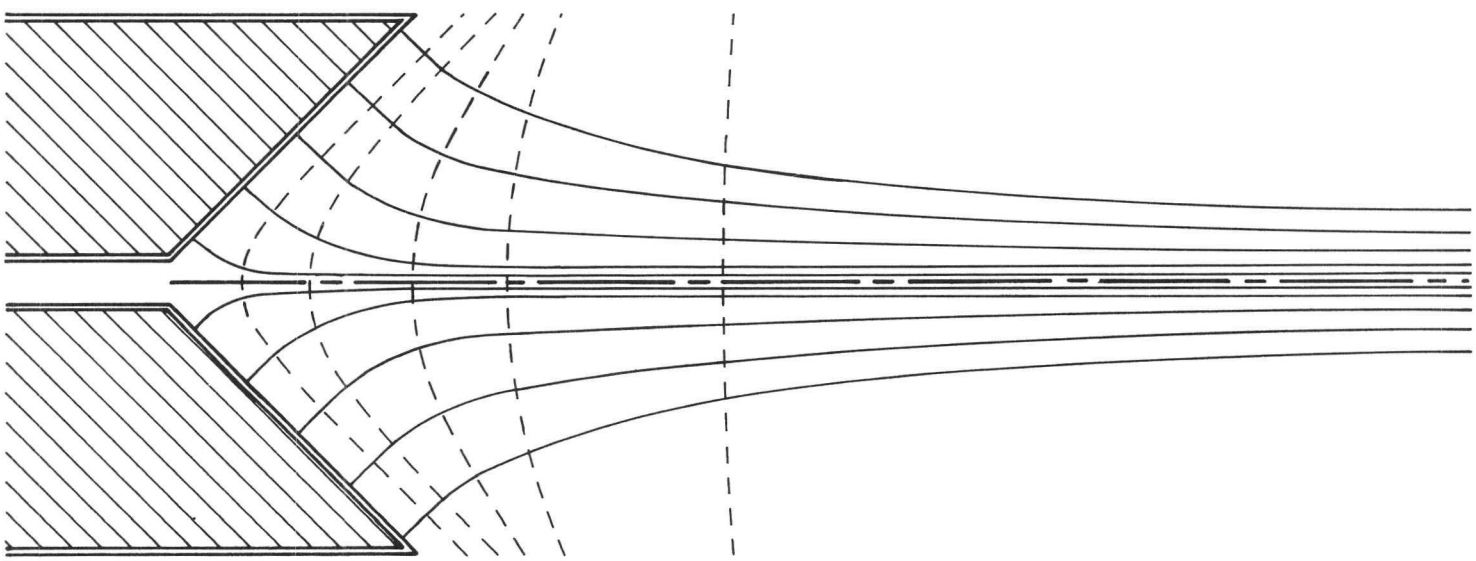

(b) Field in the vicinity of the cathode.

Figure 5.- Concluded.

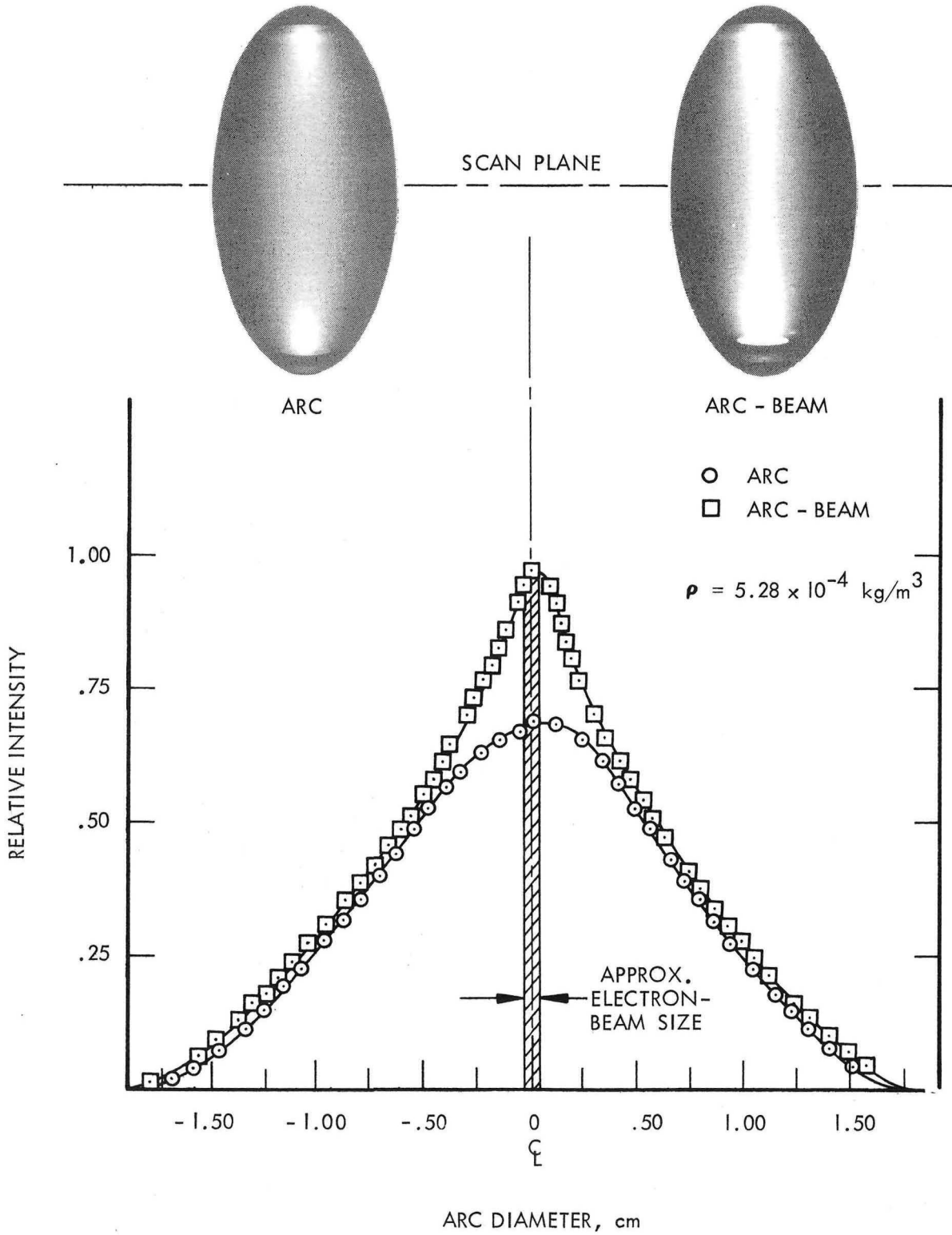

Figure 6.- Intensity profile of the arc-discharge column.

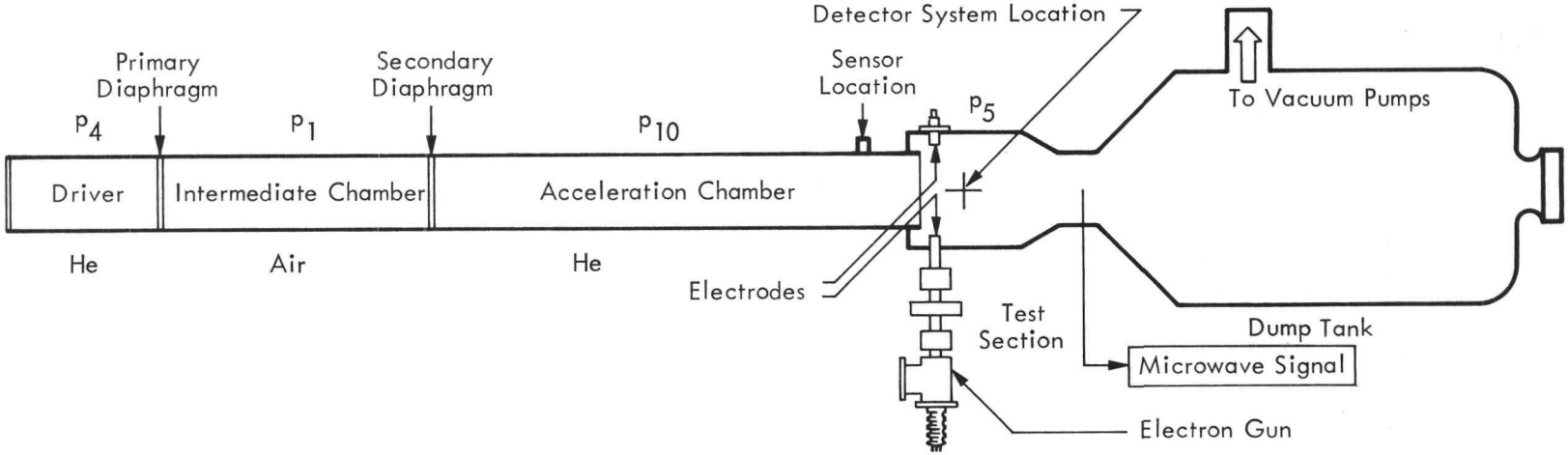

(a) Expansion tube configuration.

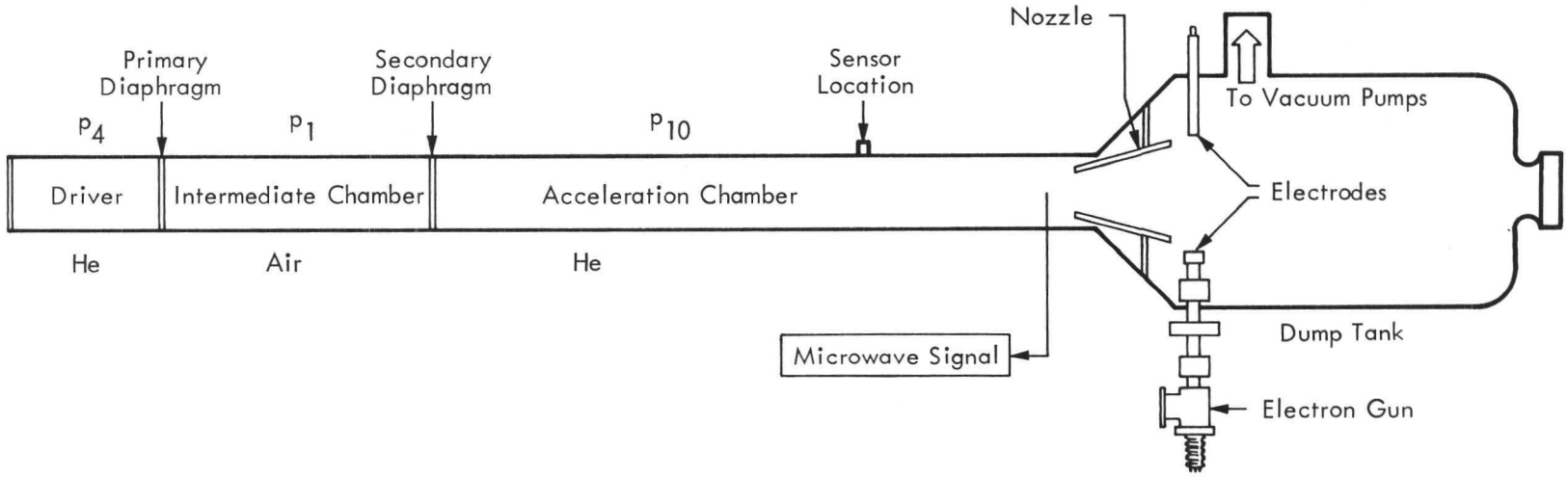

(b) Modified expansion tube configuration (expansion tunnel).

Figure 7.- Schematic diagrams of the Langley pilot model expansion tube.

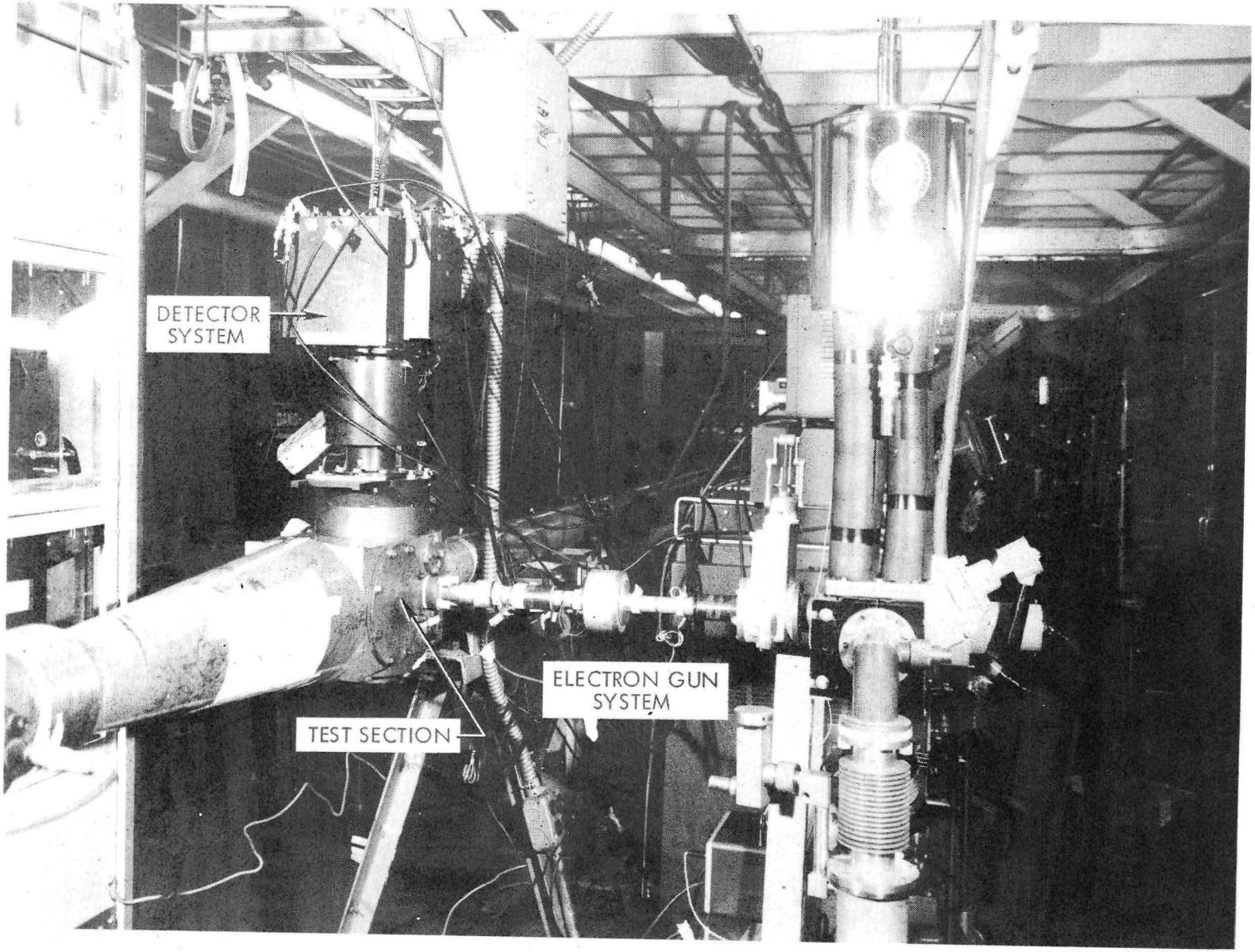

L-72-1176.1

Figure 8.- Photographs of the experimental apparatus installed in the Langley pilot model expansion tube.

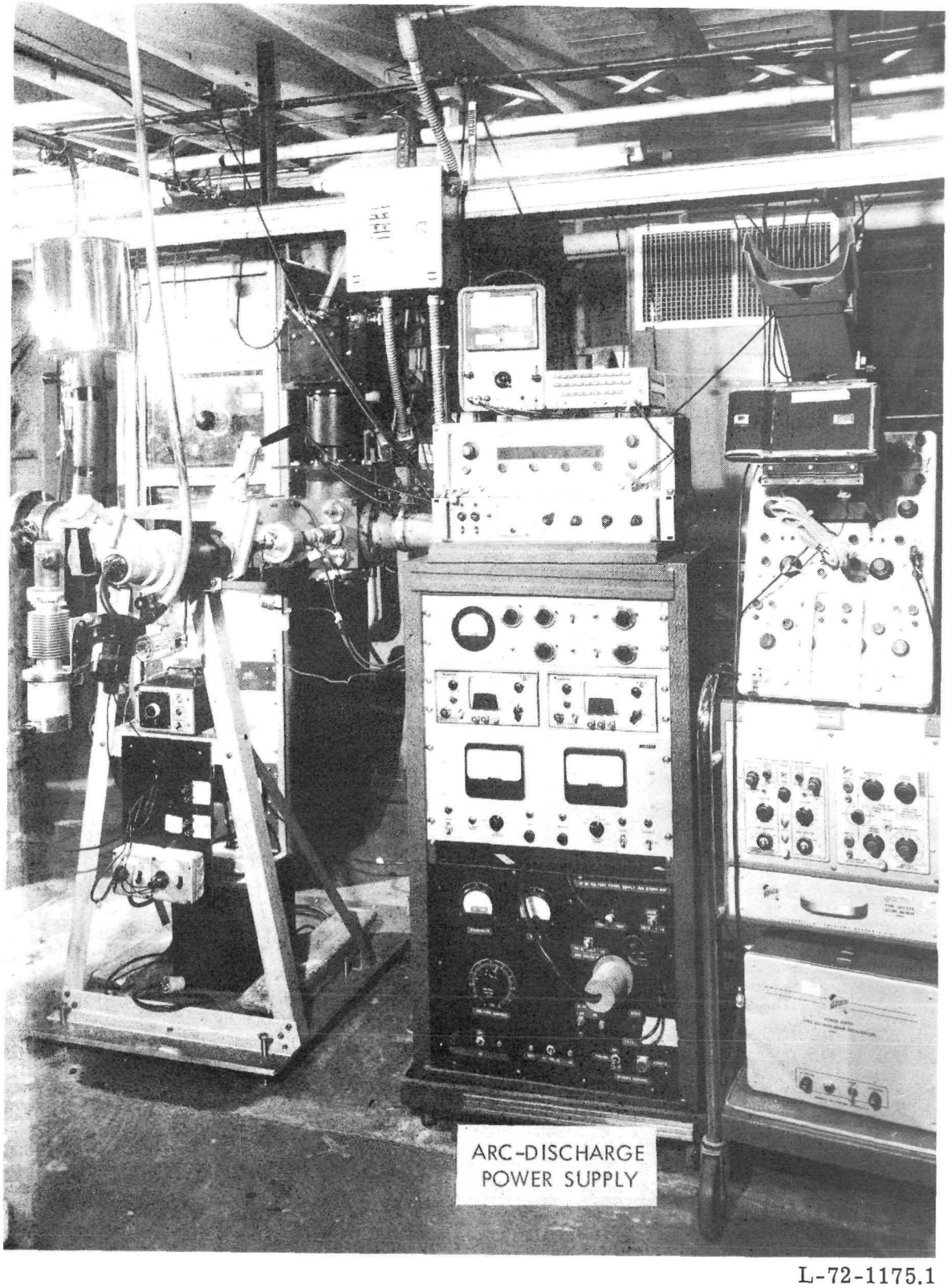

L-72-1175.1

Figure 8.- Concluded.

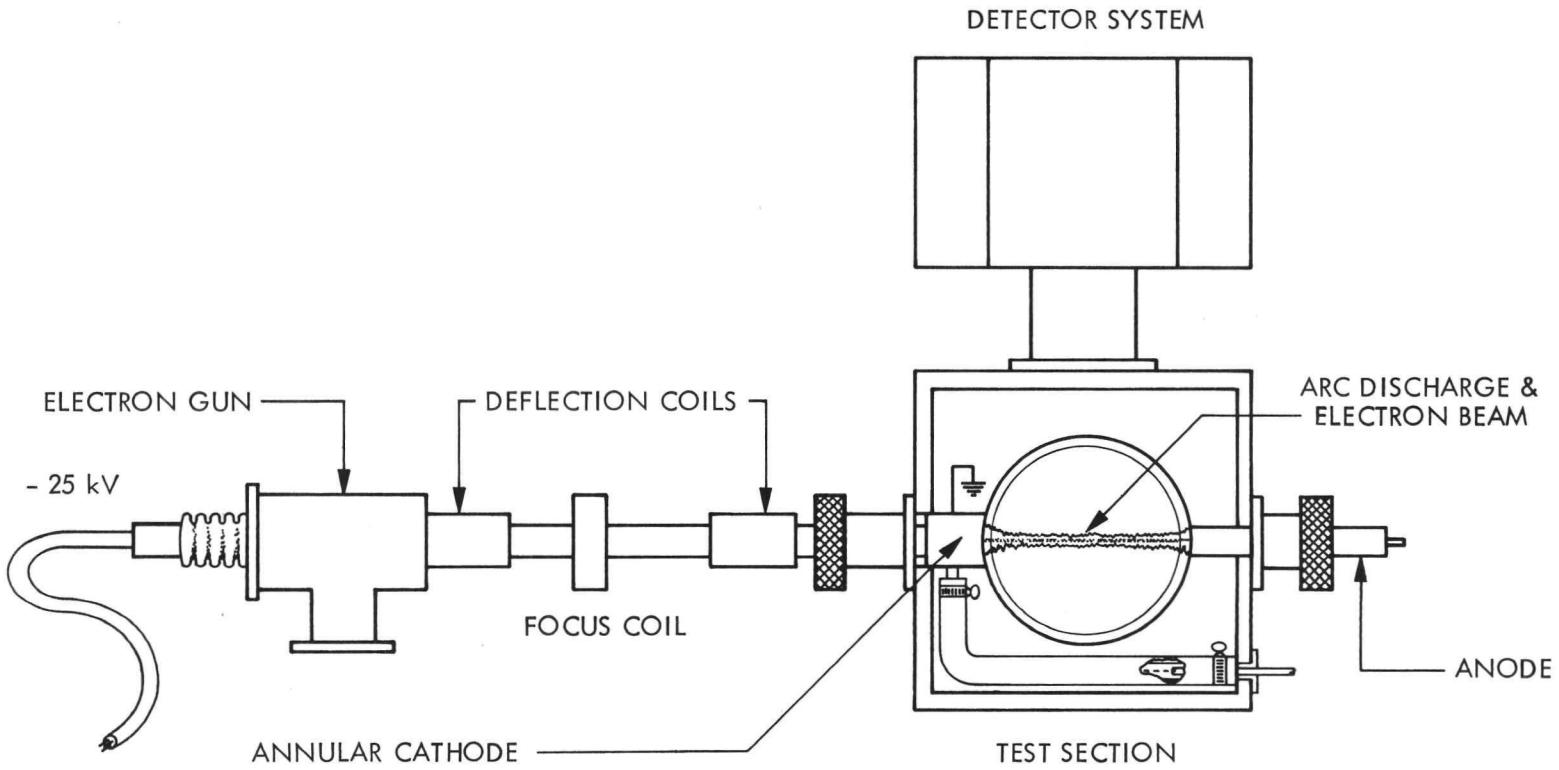

Figure 9.- A schematic diagram of the arc-discharge—electron-beam system in test section of expansion tube.

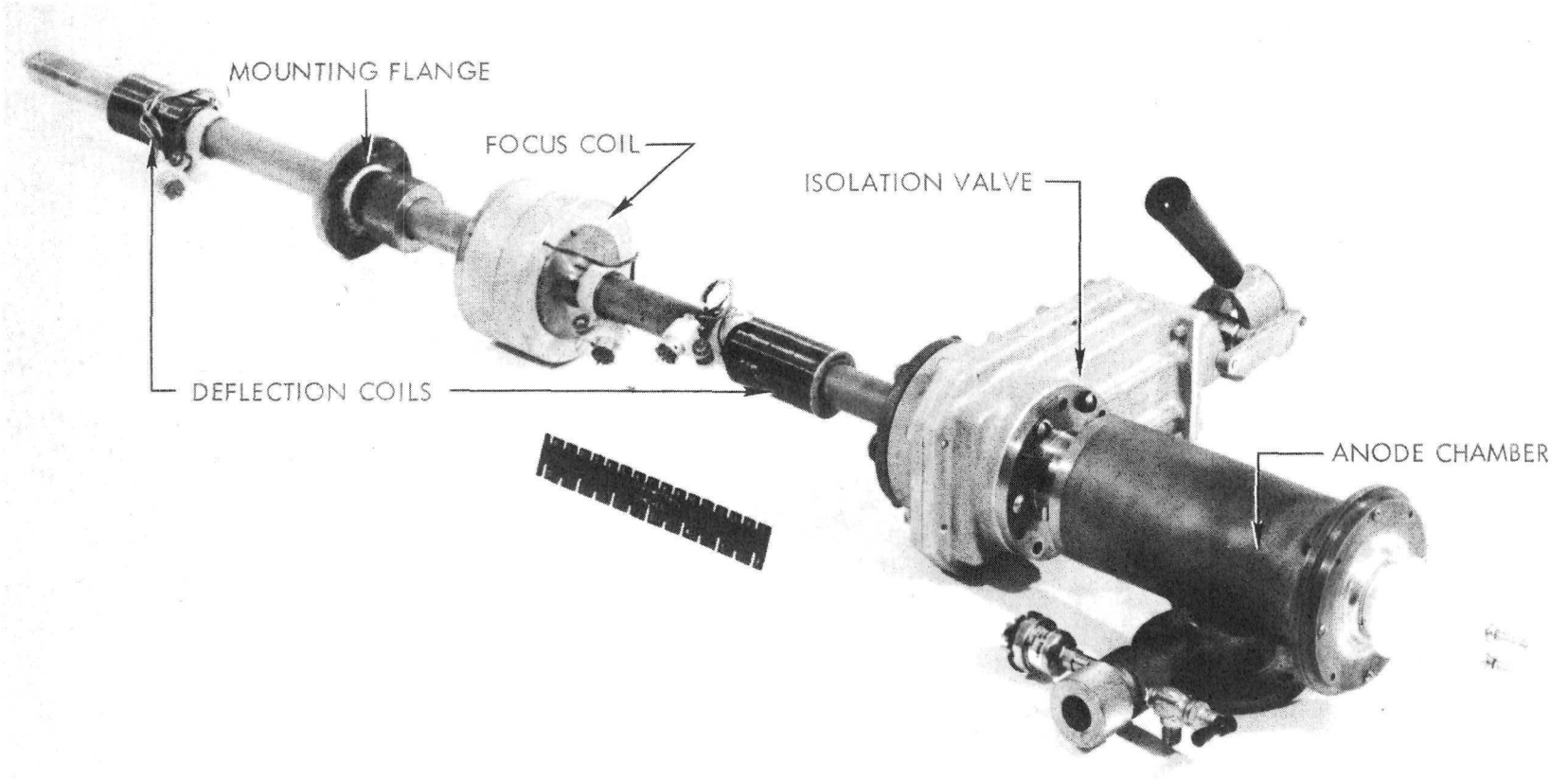

L-71-10037.1

Figure 10.- The electron gun assembly.

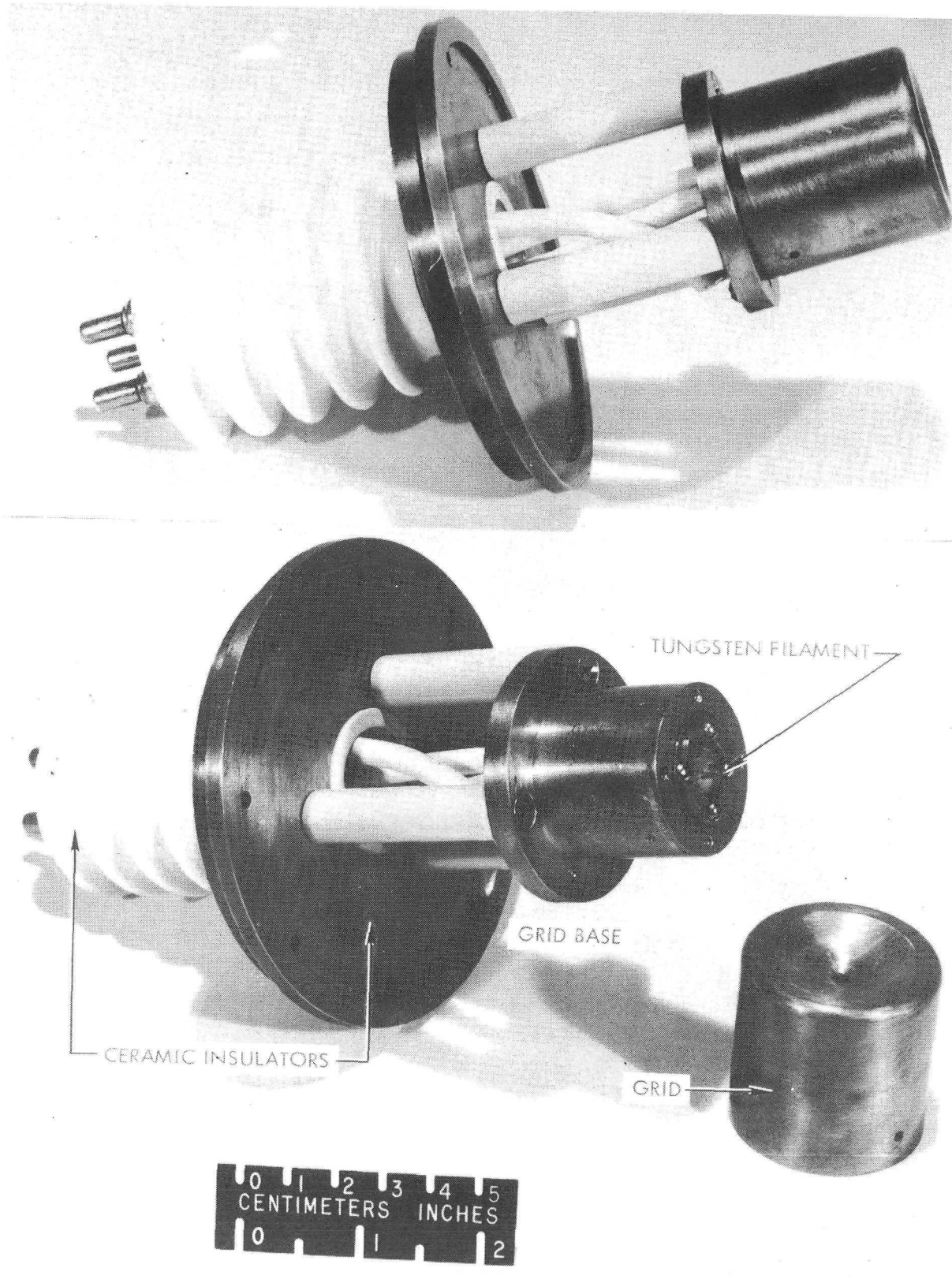

L-73-3084

Figure 10.- Concluded.

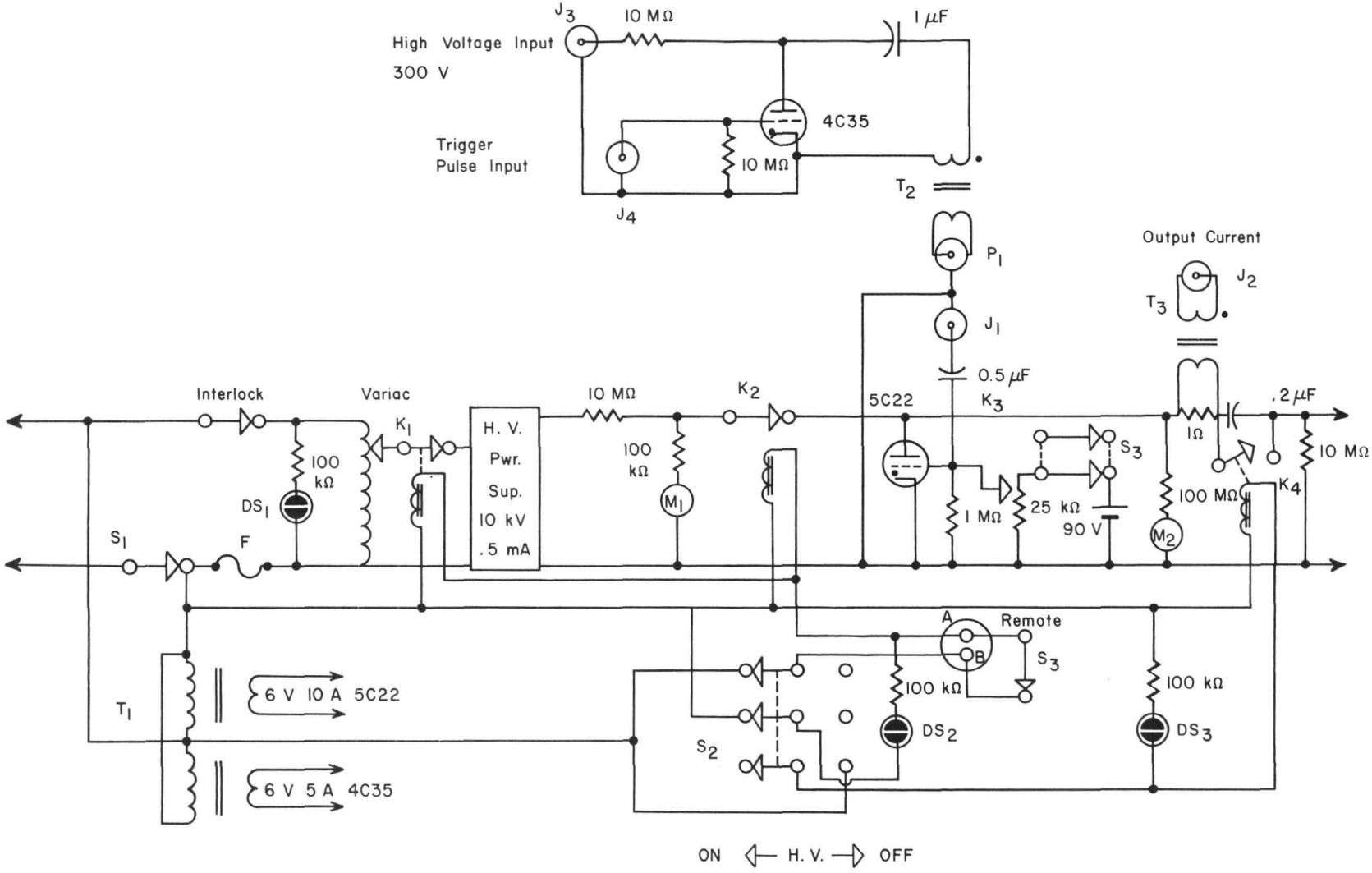

Figure 11.- Schematic diagram of arc-discharge apparatus and trigger unit.

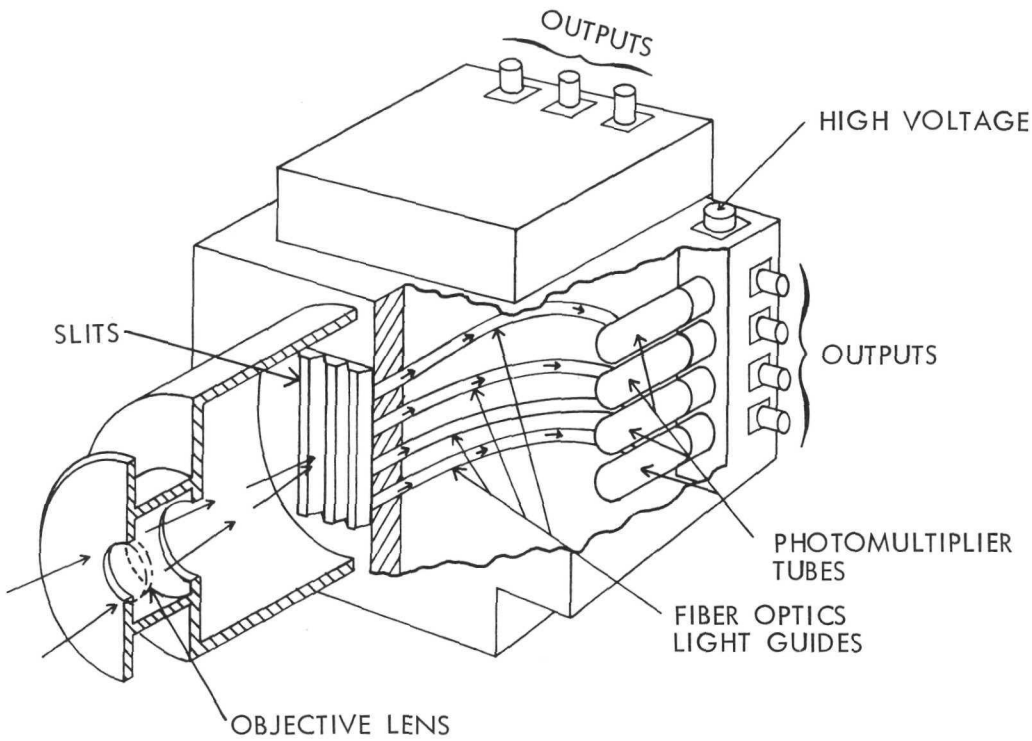

Figure 12.- A cutaway view of the detector system.

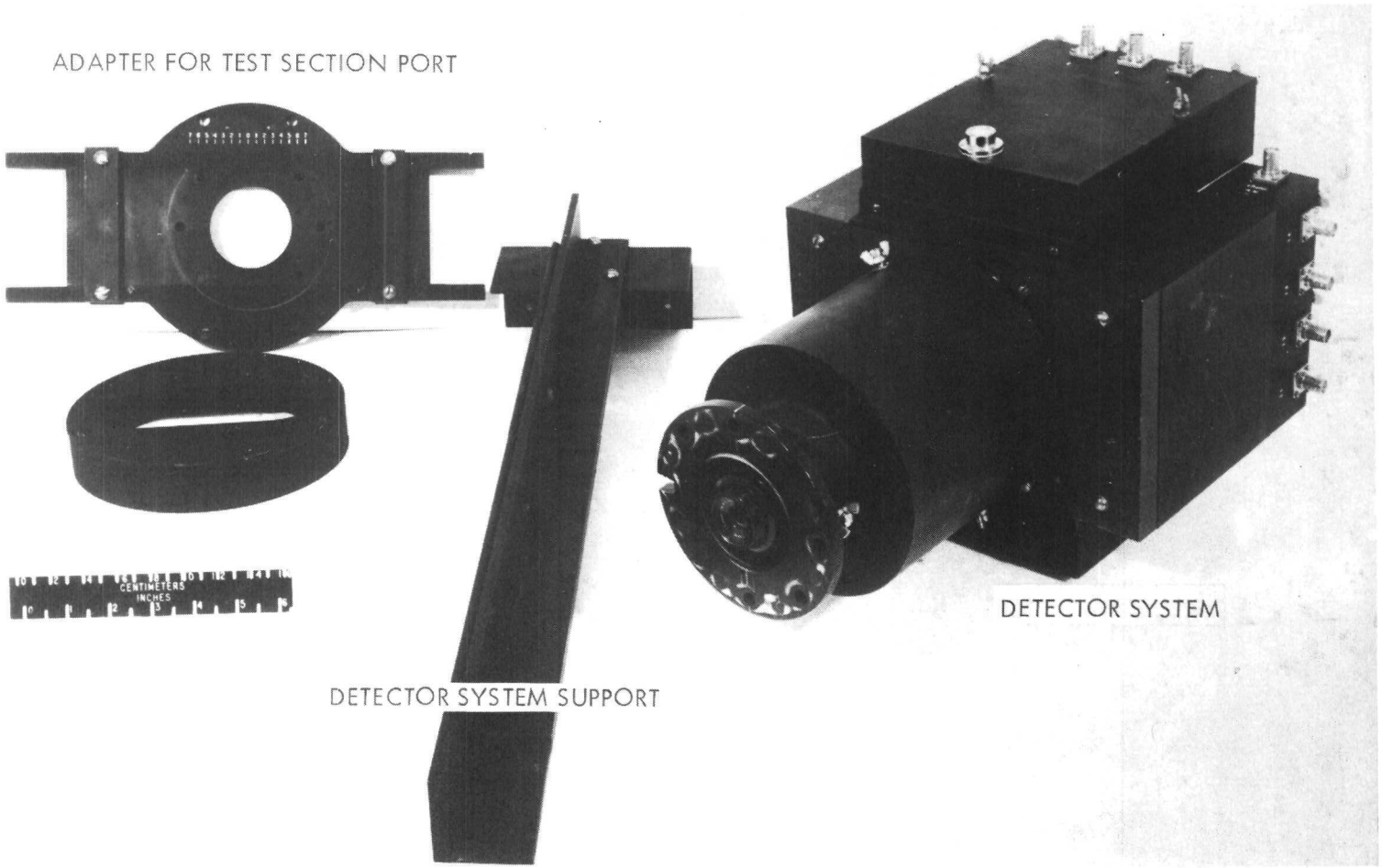

L-68-2823.1

Figure 13.- The 7 × 2 matrix detector system.

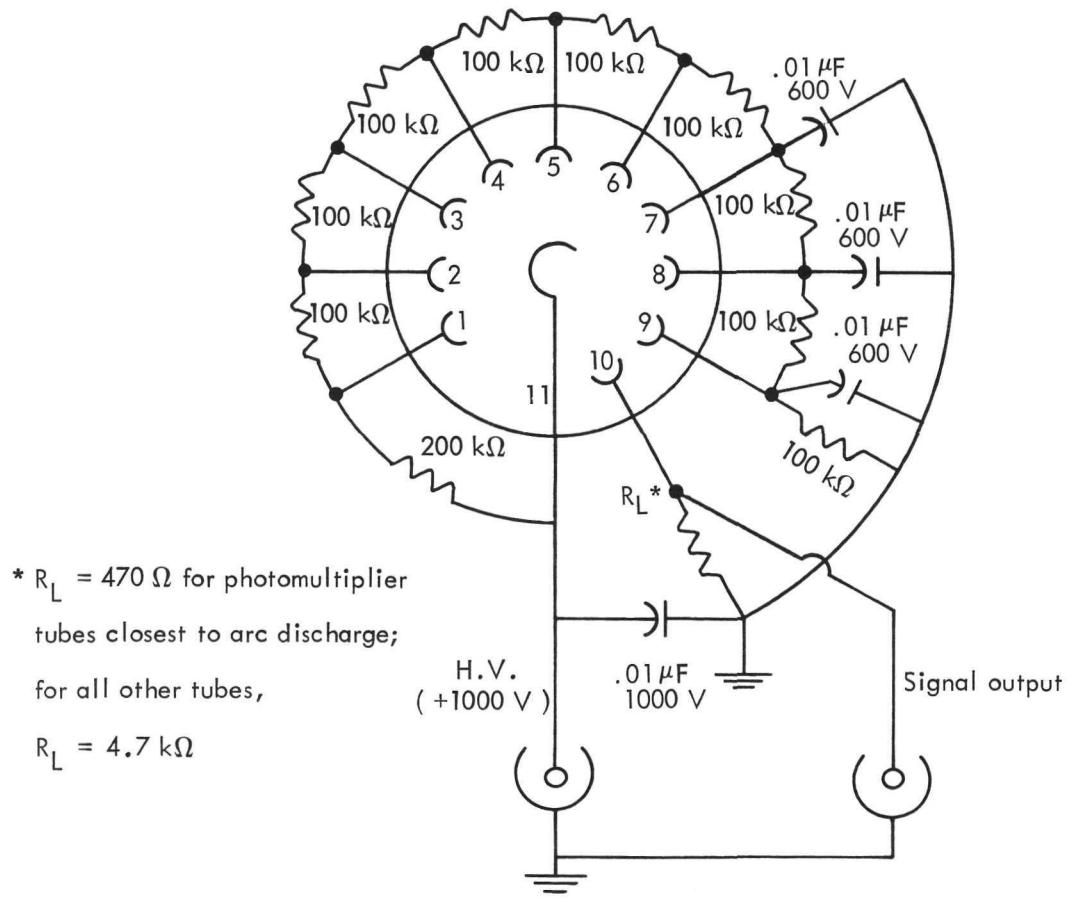

Figure 14.- A schematic diagram of the photomultiplier tube (931-A) base.

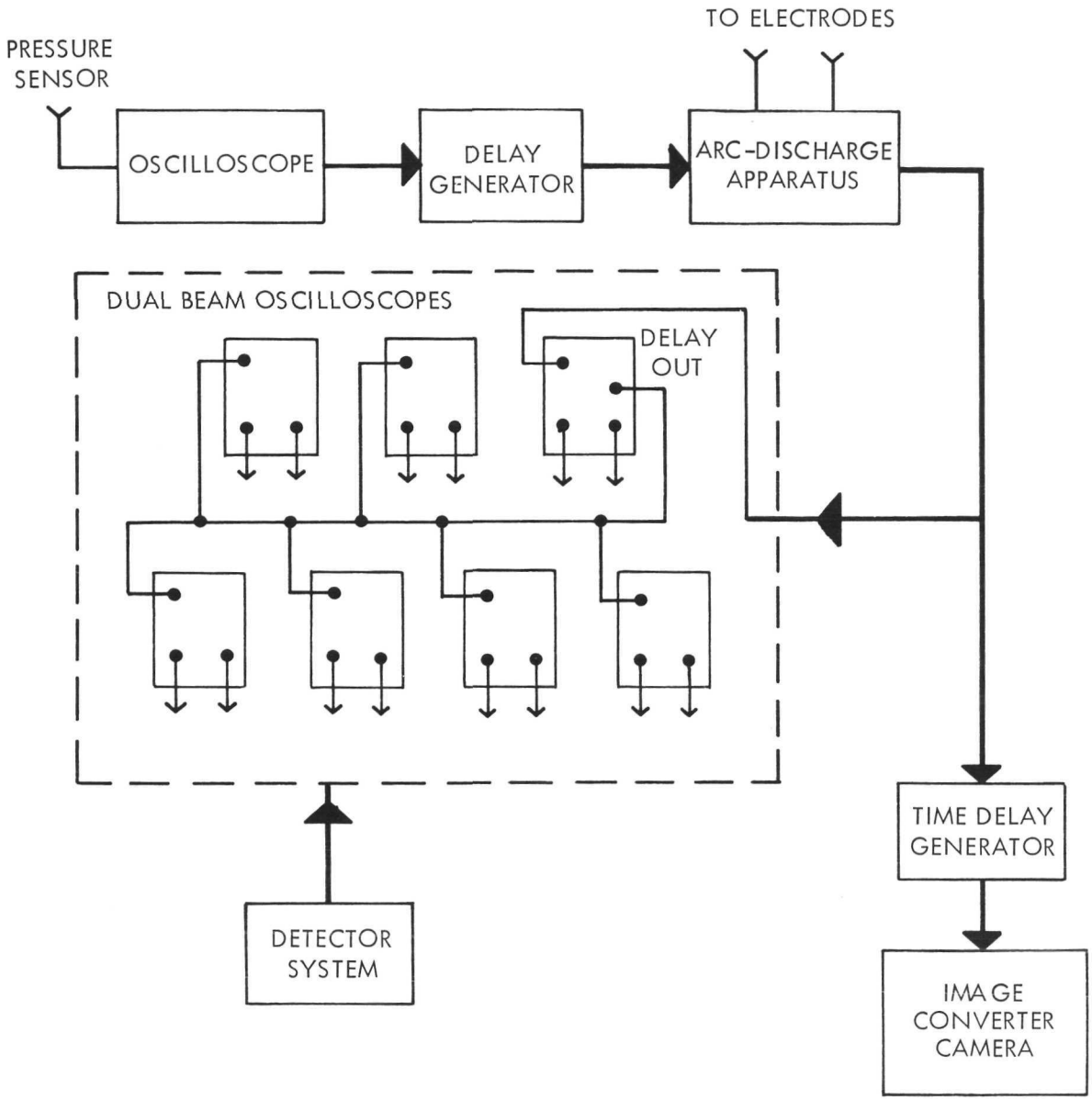

Figure 15.- Block diagram of instrument setup in the expansion tube.

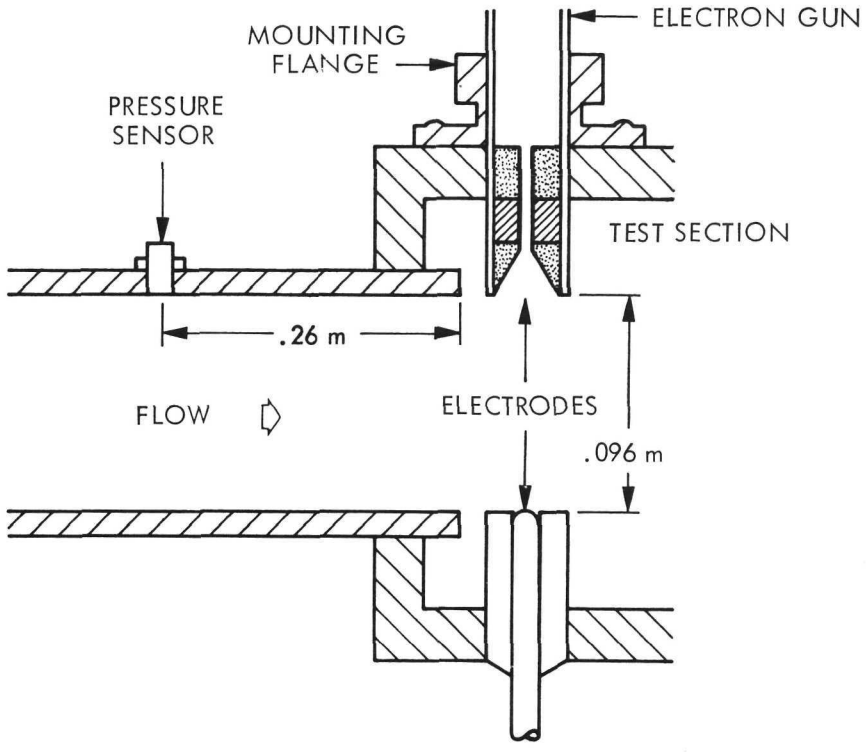

(a) Sketch of the electrode positions and location of pressure sensor.

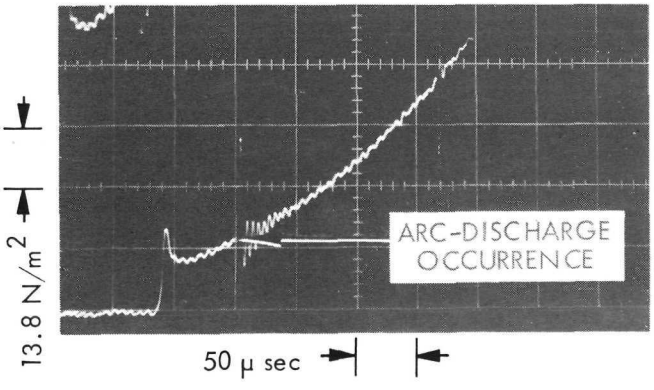

L-73-3085

(b) Oscilloscope trace of wall static pressure and arc-discharge pickup.

Figure 16.- Scheme for estimating arrival time of the flow to the test section.

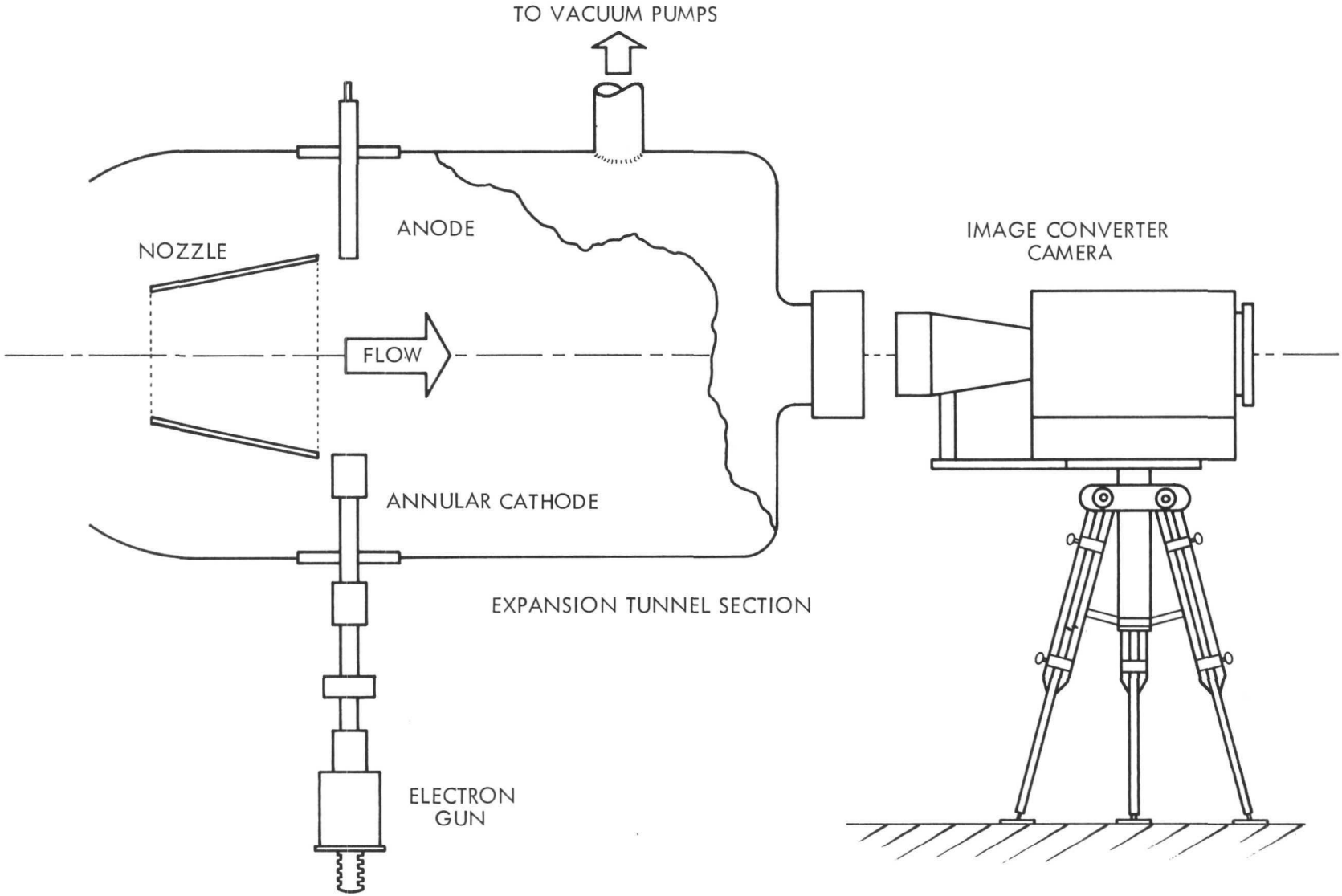

Figure 17.- Schematic diagram of the setup for photographing the arc discharge in the modified Langley pilot model expansion tube.

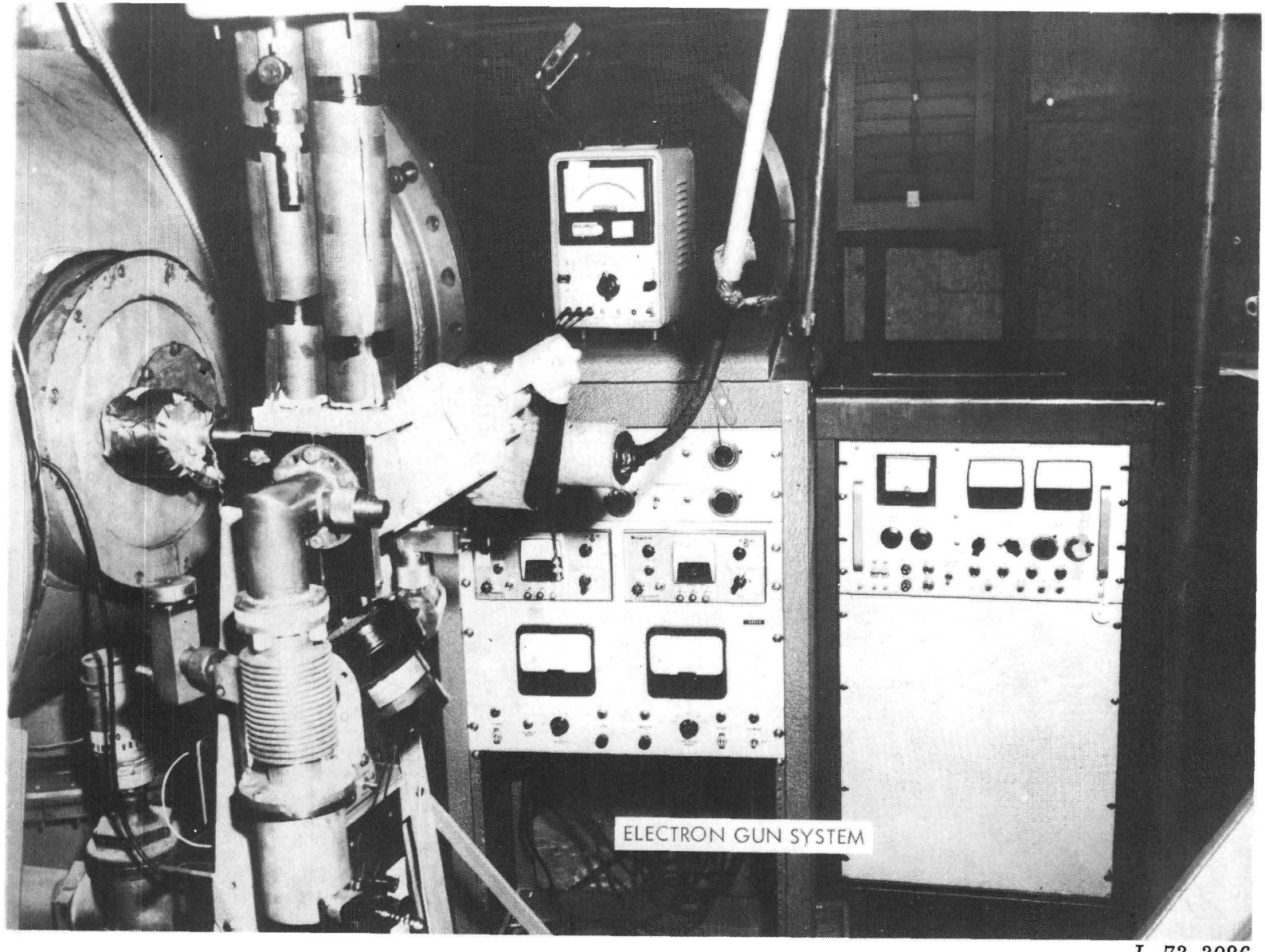

L-73-3086

Figure 18.- Installation of experimental apparatus in the modified expansion tube.

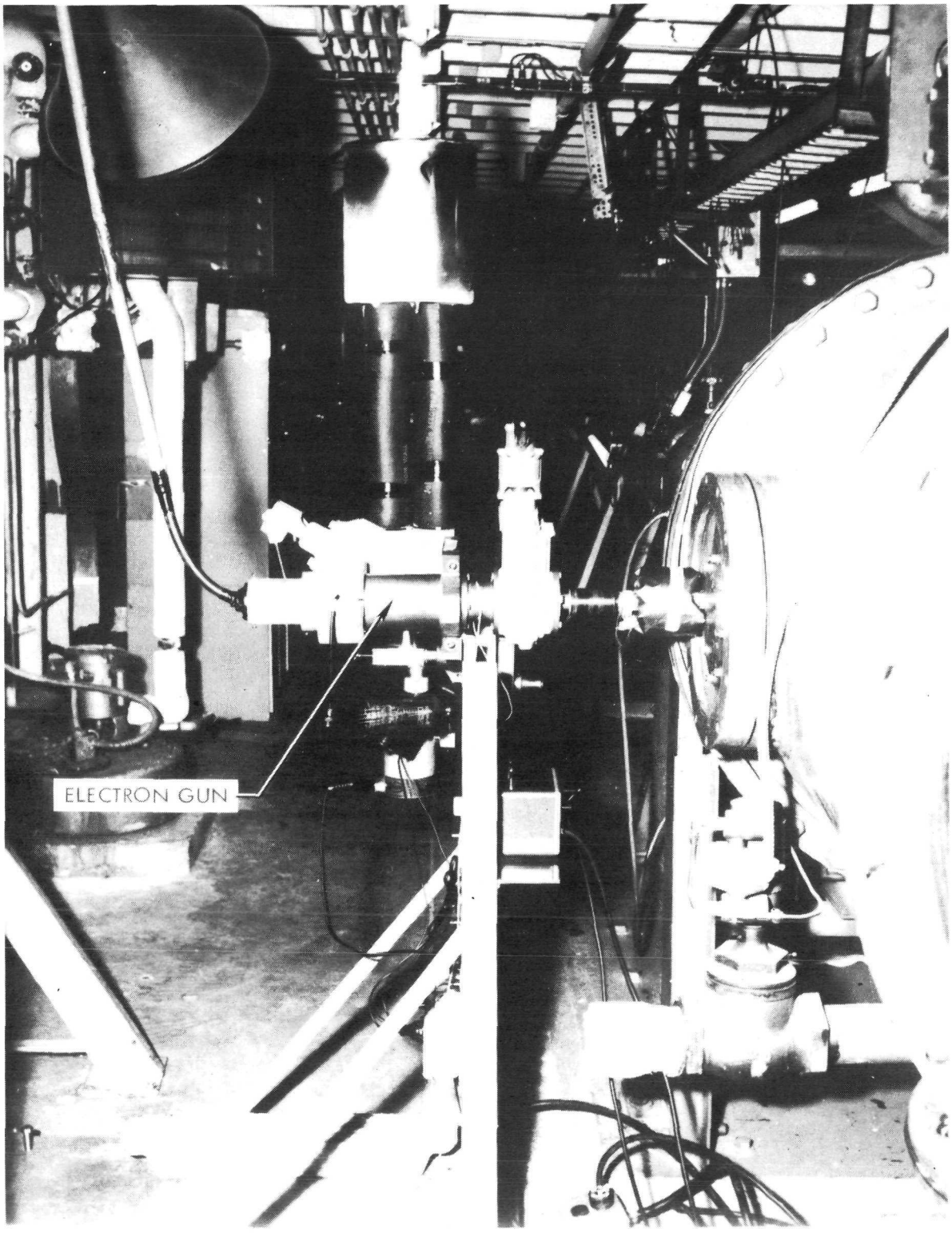

L-73-3087

Figure 18.- Concluded.

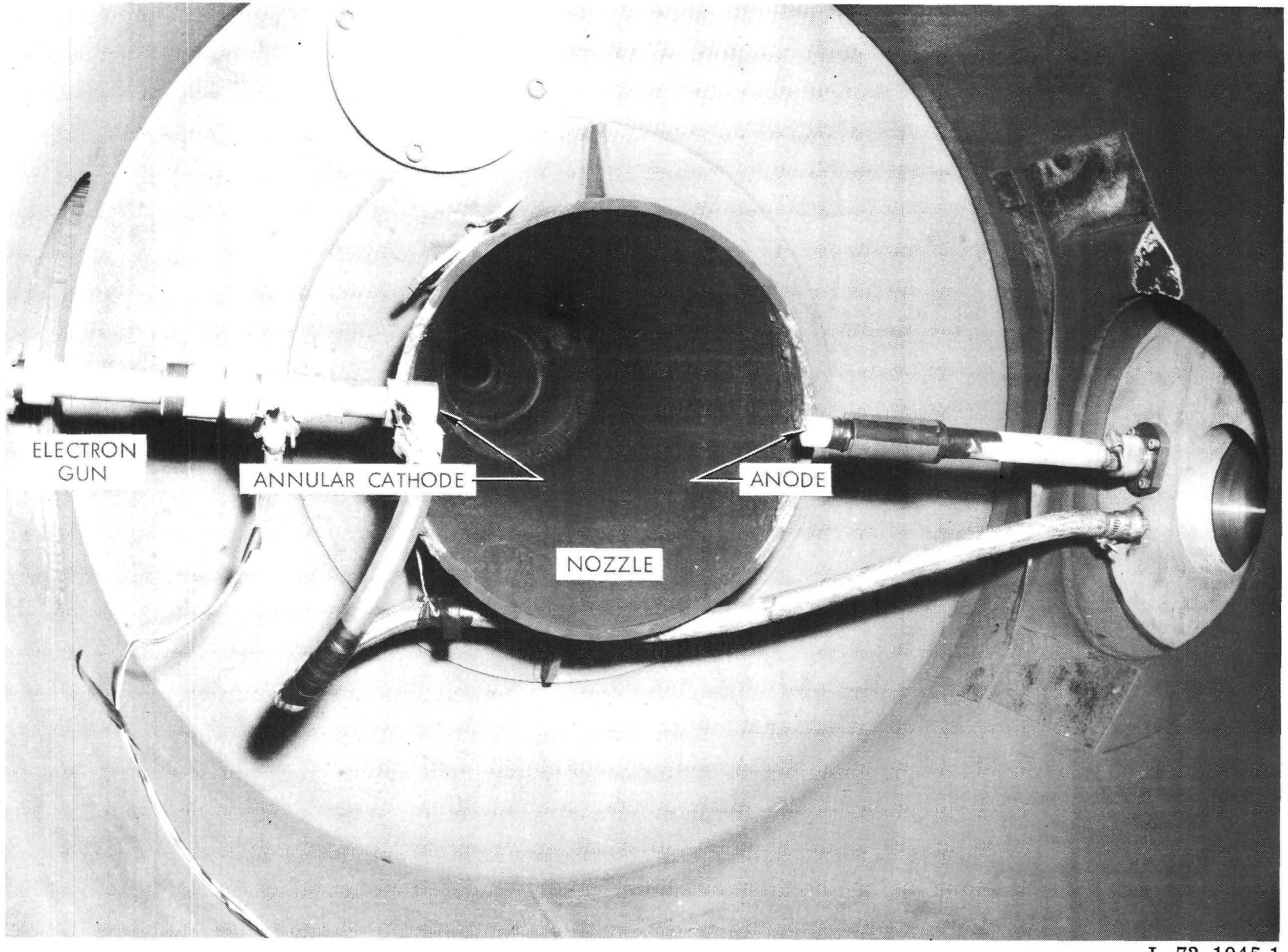

L-72-1945.1

Figure 19.- View of electrodes installed in test section of modified expansion tube.

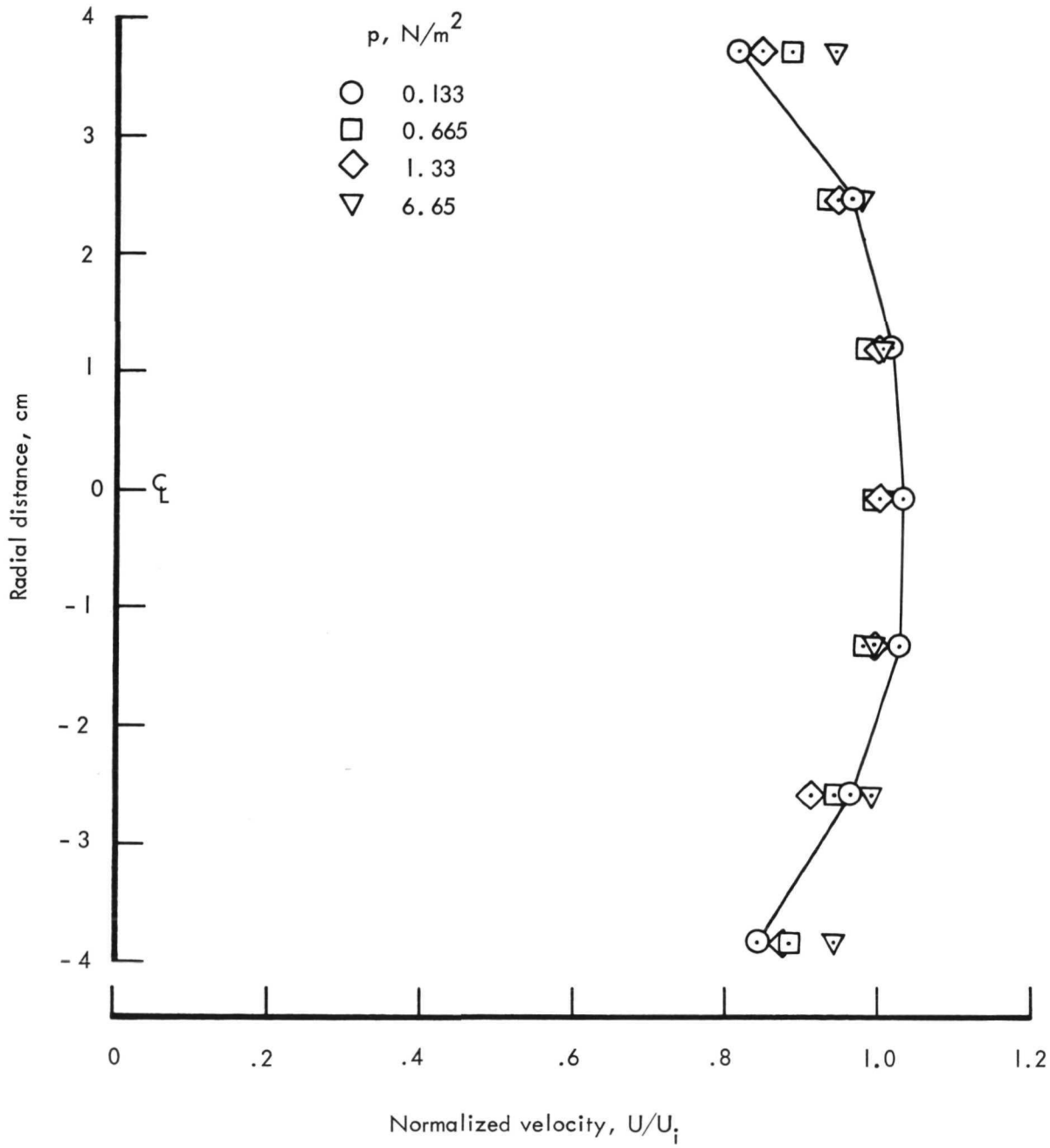

Figure 20.- Measured velocity profile normalized with respect to the helium-air interface velocity.

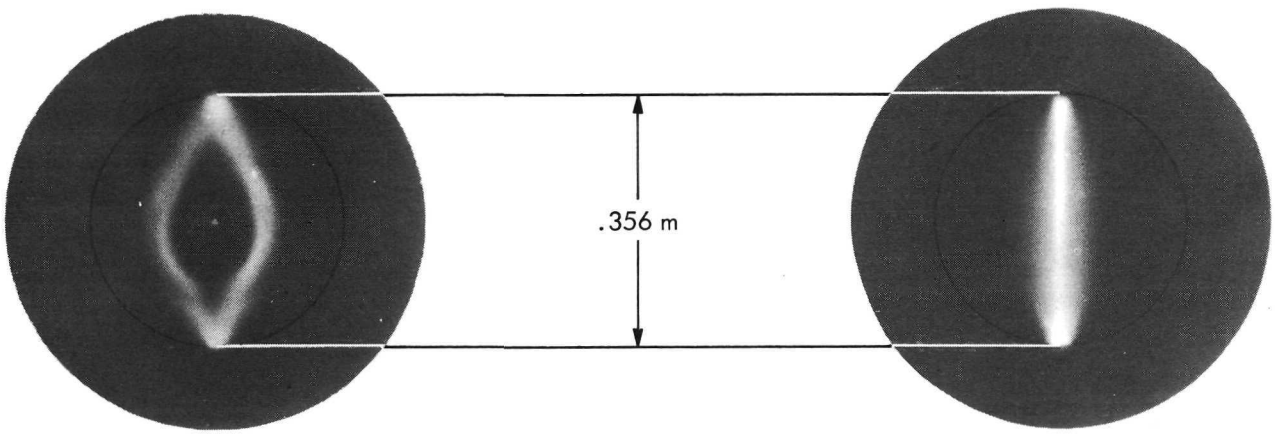

L-73-3088

(a) Arc. (b) Arc-beam.

Figure 21.- The arc and the arc-beam combination in a hypersonic flow.

NASA-Langley, 1973 —— 14 L-8815